VERSITA

OPTO-ELECTRONICS REVIEW **20**(2), 101–119

DOI: 10.2478/s11772-012-0022-1

Contactless electroreflectance spectroscopy of optical transitions in low dimensional semiconductor structures

INVITED PAPER

J. MISIEWICZ and R. KUDRAWIEC*

Institute of Physics, Wrocław University of Technology, 27 Wybrzeże Wyspiańskiego, 50-370 Wrocław, Poland

The authors present the application of contactless electroreflectance (CER) spectroscopy to study optical transitions in low dimensional semiconductor structures including quantum wells (QWs), step-like QWs, quantum dots (QDs), quantum dashes (QDashes), QDs and QDashes embedded in a QW, and QDashes coupled with a QW. For QWs optical transitions between the ground and excited states as well as optical transitions in QW barriers and step-like barriers have been clearly observed in CER spectra. Energies of these transitions have been compared with theoretical calculations and in this way the band structure has been determined for the investigated QWs. For QD and QDash structures optical transitions in QDs and QDashes as well as optical transitions in the wetting layer have been identified. For QDs and QDashes surrounded by a QW, in addition to energies of QD and QDash transitions, energies of optical transitions in the surrounded QW have been measured and the band structure has been determined for the surrounded QW. Finally some differences, which can be observed in CER and photo-reflectance spectra, have been presented and discussed for selected QW and QD structures.

Keywords: contactless electroreflectance, quantum wells, quantum dots, optical transitions.

Contents

1. Introduction

Electro-modulation (EM) spectroscopy is known as a very powerful absorption-like technique to study various material issues in different semiconductor heterostructures including quantum wells, quantum dots and others quantum systems [1–5]. The basic idea of this technique is to measure the derivative of the reflectance spectrum with respect to modulating electric field. In general, the electric field modulation inside the sample can be achieved in several ways, including contact and contactless modes. The contact mode called electroreflectance (ER) needs to apply an electric field directly on the semiconductor, either through a Schottky barrier or a semiconductor/electrolyte junction. This approach is destructive for samples and, therefore, another approaches like photo-reflectance (PR) and contactless electroreflectance (CER) are more favoured. In the case of PR, the band bending modulation (i.e., the surface electric field modulation) takes place due to the photovoltaic effect, which is induced by photo-generated carriers. Unfortunately, this carriers lead to an unwanted photoluminescence (PL) signal which can complicate measurements of PR spectra very significantly. This inconvenience is overcome in CER spectroscopy and, therefore, this technique is often recommended for the non-destructive characterization of semiconductor heterostructures. The band bending modu- lation in CER spectroscopy is realized in contactless mode by using a capacitor system with one electrode which is semi-transparent for light [5,6]. The periodic modulation of a built-in electric field inside the sample produces sharp spectral features at photon energies which correspond to inter-band transitions. Due to the Franz-Keldysh effect, CER spectroscopy can be also applied to investigate the built-in electric field and the Fermi-level position in semiconductor heterostructures [7–10]. For recent years CER spectroscopy was widely applied to study various material issues in different semiconductor materials and heterostructures [7–28]. In this paper we present both main principles of CER spectroscopy and examples of our recent application of CER spectroscopy to study quantum wells, quantum dots/dashes, and other quantum structures.

*e-mail: robert.kudrawiec@pwr.wroc.pl

2. Experiment

The condition to obtain CER signal is the existence of a built-in electric field inside the sample under investigation. This condition is usually fulfilled in majority semiconductor structures since such samples possess a surface electric field or a built-in electric field at internal interfaces. This field results from different level of intentional (or unintentional) doping in individual layers as well as different concentrations of native point defects in these layers. It is worth noting that it is usually more difficult to obtain such conditions in narrow gap semiconductors at room temperature and, therefore, the modulation of built-in electric field in such structures can be inefficient at room temperature.

Both the bright and dark experimental configurations can be applied to measure CER spectra [29]. In general, the classical approach to measure electro-modulation spectra (including the CER ones) is the dark configuration [1–4] where the sample is illuminated with monochromatic light. Recently, the "bright" configuration is widely applied to measure PR and CER spectra [10–18,29,30]. In this review paper this experimental configuration is described and applied to study optical properties of low dimensional semiconductor structures.

2.1. Experimental set-up

Figure 1 shows an experimental set-up for CER measurements in the "bright" experimental configuration [29,30]. The typical capacitor used for CER measurements is shown in Fig. 2. The sample is mounted inside such a capacitor on the bottom electrode by using a conductive glue. The front electrode is made from a wire mesh, is semi-transparent for light and is separated from the sample surface by a spacer. Thus, there is no electric contact between the top electrode and the sample surface. It means that the sample does not conduct any currents and the external electric field is able to change the carrier distribution inside the sample. Due to no electric contact between the electrode and the sample the

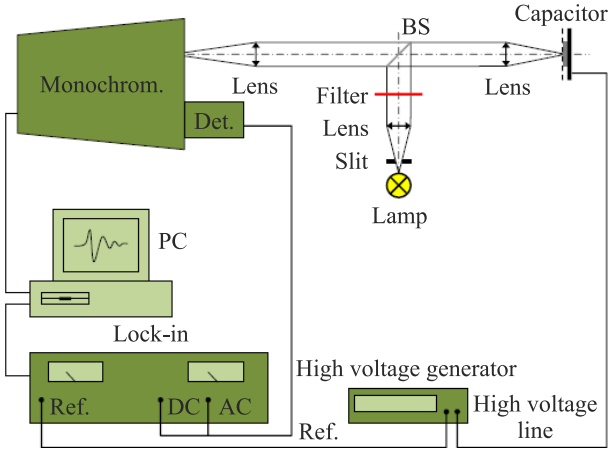

Fig. 1. Experimental set-up for contactless electroreflectance measurements in "bright" configuration (BS-beam splitter; PC-personal computer).

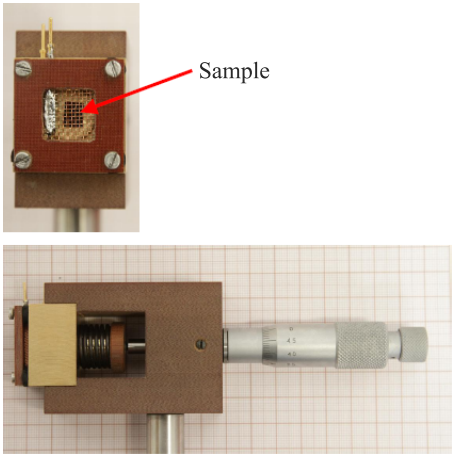

Fig. 2. Capacitor used to contactless electroreflectance measurements.

voltage drop appears mainly in the air gap between the top electrode and the sample. The limit for the applied voltage is the electric breakdown in this air gap. A generator of a square AC voltage is used to create the AC field inside the capacitor. A maximum peak-to-peak alternating voltage of 2–3 kV with the frequency of 280 Hz is usually used for the modulation when the spacer between the electrode and the sample is ~0.5 mm.

2.2. Data analysis

In CER spectroscopy we measure changes in reflectance spectrum which are induced by changes in the built-in electric field inside the investigated sample. In order to extract maximum information from experimental data, an appropriate analysis of spectral features has to be performed. In general, changes in reflectance spectrum are related to the perturbation of the dielectric function ($\varepsilon = \varepsilon_1 + i\varepsilon_2$) and they are described by the following equation [1–3]

$$\frac{\Delta R}{R} = \alpha(\varepsilon_1, \varepsilon_2)\Delta\varepsilon_1 + \beta(\varepsilon_1, \varepsilon_2)\Delta\varepsilon_2, \qquad (1)$$

where α and β are the Seraphin coefficients related to the dielectric function, and $\Delta\varepsilon_1$ and $\Delta\varepsilon_2$ are related by Kramers-Kronig relations. The detailed line-shape of CER features related to optical transitions can be discussed in terms of electro-modulation mechanisms which can be classified into three categories depending on the relative strengths of characteristic energies [31]. In the low-field regime $|\hbar\Omega| \leq \Gamma$, where Γ is the broadening parameter and $\hbar\Omega$ is the electro-optic energy given by Eq. (2)

$$(\hbar\Omega)^3 = \frac{q^2\hbar^2F^2}{2\mu}. \qquad (2)$$

In the above equation F is the electric field and μ is the reduced interband mass in the direction of the field. In the intermediate-field case, when $|\hbar\Omega| \geq \Gamma$ and $qFa_0 << E_g$ (a_0 is the lattice constant), Franz-Keldysh oscillations (FKO)

appear in EM spectra. In the high-field regime the electro-optic energy is much greater than the broadening Γ but $qFa_0 \approx E_g$ so that Stark shifts are produced. Theoretical descriptions of the spectral features observed in the EM spectra are discussed in detail in Refs. 31–37. The most important conclusions are presented below.

Low field limit: Electroreflectance spectra of simple, lightly-doped systems, measured under low field conditions can often be modelled using Aspnes' third derivate functional form [31], so-called Lorentzian line shape

$$\frac{\Delta R}{R} = \mathrm{Re}[Ae^{i\theta}(E - E_0 + i\Gamma)^{-m}], \tag{3}$$

where E_0 is the critical point (*CP*) energy, Γ is the broadening parameter ($\Gamma \sim \hbar/\tau$), A and θ are the amplitude and phase factor, respectively. The term m refers to the type of *CPs*, i.e., the nature of optical transitions, namely: m = 2, 2.5 and 3 for an excitonic transition, a three-dimensional (3D) *CP* one-electron transition and a two-dimensional (2D) *CP* one--electron transition, respectively. This formula is appropriate at low temperatures for high quality structures. At room temperature, the Lorentzian dielectric function can be inappropriate and Eq. (3) should be replaced by more general equation [2,3]. For a better visualization of optical transitions observed in CER spectra the modulus of CER resonance can be plotted. Such a modulus is defined by Eq. (4)

$$|\Delta\rho(E)| = \frac{|A|}{[(E - E_0)^2 + \Gamma^2]^{m/2}}, \tag{4}$$

where A, E_0, , and Γ parameters are taken from the fitting procedure by Eq. (3).

Intermediate field limit: When the low-field criteria are not satisfied, but $eFa_0 << E_g$, the dielectric function can exhibit Franz-Keldysh oscillations. Although the exact form of $\Delta R/R$ for the intermediate-field case with the broadening is quite complicated, Aspnes and Studna [32] have derived a relatively simple equation

$$\frac{\Delta R}{R}(E) \propto \frac{1}{E^2 (E - E_g)} \exp\left[-2(E - E_g)^{1/2} \frac{\Gamma}{(\hbar\Omega)^{3/2}}\right] \times \cos\left[\frac{4}{3}\frac{(E - E_g)^{3/2}}{(\hbar\Omega)^{3/2}} + \chi\right], \tag{5}$$

where E is the energy, E_g is the energy gap for the considered optical transition, $\hbar\Omega$ is the electro-optic energy defined by Eq. (2), Γ is the line-width, and χ is the arbitrary phase factor. From the above equation, the position of a nth extreme in the Franz-Keldysh oscillation is given by

$$n\pi = \frac{4}{3}\left[\frac{E_n - E_g}{\hbar\Omega}\right]^{3/2} + \chi, \tag{6}$$

where E_n is the photon energy of the nth extreme [33]. A plot $(4/3\pi)(E_n - E_g)^{3/2}$ *vs.* the index number n will yield a straight line with slope $(\hbar\Omega)^{3/2}$. Therefore, the electric field F can be directly obtained from the period of FKO if μ [i.e., the electron-hole reduced mass, see Eq. (2)] is known.

3. Results

The application of CER spectroscopy to study low dimensional heterostructures allows to investigate various material issues like (i) the built-in electric field including the Fermi-level position [7–10,15], (ii) the band-offset at semiconductor interfaces [11–14], (iii) the homogeneity of low dimensional systems [16], (iv) the carrier localization effect including the Stokes shift [17], as well as other issues/effects [18]. Some examples of the application of CER spectroscopy to study selected material systems/heterostructures are presented below.

3.1. Quantum wells

In QW structures energies of optical transitions between both the ground and excited states as well as energies of QW barriers can be measured by CER due to its absorption-like character. For well- known QW systems CER spectroscopy can be used to verify the QW width and/or content since energies of QW transitions (both the ground and excited state transitions) are very sensitive to these parameters. For a QW containing new semiconductor materials CER spectroscopy can be used to determine the band gap discontinuity at QW interfaces (the band offset) as well as the effective masses of carriers. For these purposes the QW width and alloy content have to be determined very carefully for the investigated samples using structural methods like X-ray diffractions and/or the cross section transmission electron microscopy. In addition, broadenings of CER resonances are very sensitive to the structural quality of the investigated QWs, i.e., the roughness of QW interfaces and alloy content inhomogeneities [16,17]. In this part we focus on the application of CER spectroscopy in order to study the number of confined states in QWs and band gap discontinuities at QW interfaces.

Figure 3 shows room temperature CER spectrum measured for a $Ga_{0.47}In_{0.53}As/Al_{0.24}Ga_{0.23}In_{0.53}As$ QW grown on InP substrate [38]. The strongest CER signal at ~1.06 eV is associated with the photon absorption in $Al_{0.24}Ga_{0.23}In_{0.53}As$ bulk-like QW barriers (note that in this figure this signal is divided by a factor of 5 for a better visualization of the other part of CER spectrum). The CER resonances below the AlGaInAs-related transition are associated with the optical transitions in the $Ga_{0.47}In_{0.53}As$ QW. These resonances have been fitted by Eq. (3) with m = 2 which corresponds to an exciton transition. The fitting curve is shown by a thick grey line in Fig. 3 together with the moduli of the individual resonances (dashed lines) obtained according to Eq. (4). The identification of the resonances is possible on the basis of the calculations performed in the framework of the effective mass approximation. Relevant details of our theoretical calculations can be found in Ref. 38. The nota-

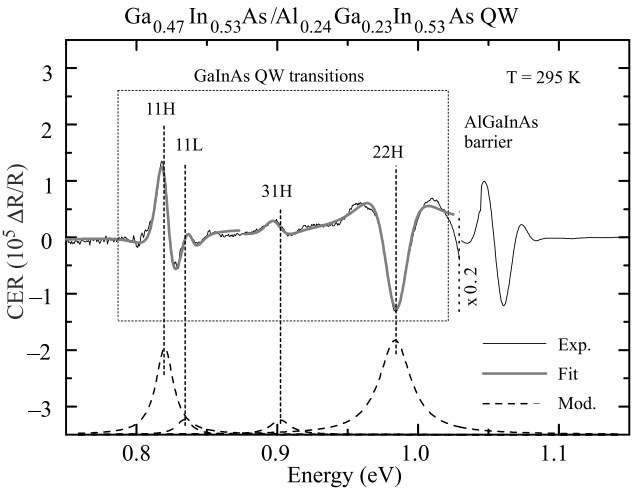

Fig. 3. Room temperature contactless electroreflectance spectrum of 7-nm wide $Ga_{0.47}In_{0.53}As/Al_{0.24}Ga_{0.23}In_{0.53}As$ QW together with fitting curves (thick grey line) and the moduli of the individual resonances (dashed lines).

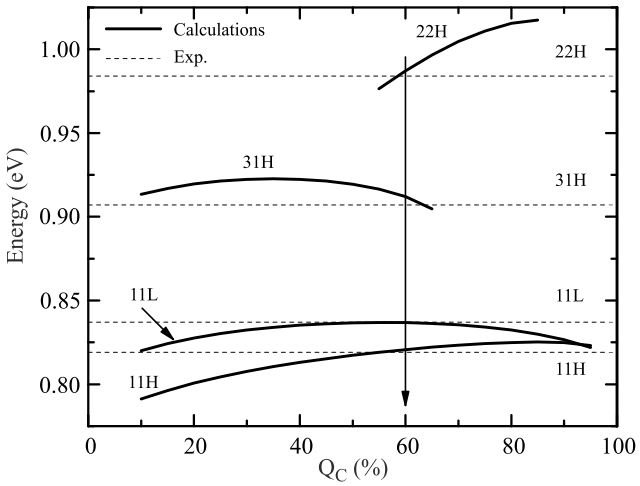

Fig. 4. Method used to analyse the Q_C in $Ga_{0.47}In_{0.53}As/Al_{0.24}Ga_{0.23}In_{0.53}As$ QW, i.e., a comparison of the experimental data (horizontal dashed lines) with theoretical predictions obtained for various Q_C values (solid curves).

tion *kl*H(L) in Fig. 3 denotes the transition between the *k*-th heavy-hole (light-hole) valence subband and the *l*-th conduction subband. The resonance at the lowest energy is related to the 11H transition, which is the fundamental transition for this QW structure. In addition to the 11H transition, the spectrum shows the 11L transition (i.e., the lowest energy transition for light-holes) and transitions between excited QW states like 31H and 22H transitions.

The comparison of energies of QW transitions extracted from CER measurements with these obtained from theoretical calculations, which are performed for various conduction band offsets (Q_C), allows us to determine the band structure for investigated QWs. An example of such a comparison is shown in Fig. 4 where the horizontal dashed lines represent energies of QW transitions extracted from CER measurements and the thick solid curves are theoretical predictions of QW transitions for various Q_C, which is defined by Eq. (7) as

$$Q_C = \frac{\Delta E_C}{(\Delta E_C - \Delta E_V)} \times 100\%, \tag{7}$$

where ΔE_C and ΔE_V are the conduction- and valence-band discontinuities at the heterojunction for unstrained materials (individual bulk alloys). In the case of $Ga_{0.47}In_{0.53}As/Al_{0.24}Ga_{0.23}In_{0.53}As$ QW grown on InP substrate the "unstrained" Q_C is the same as the "strained" Q_C since both the QW and barrier layers are lattice matched to the InP substrate. It is worth noting that in this approach the Q_C between QW (ternary alloy) and barrier (quaternary alloy) material is analysed. More universal approach is to determine the Q_C between the QW material (ternary or quaternary alloy) and the binary compound, which is used as the substrate. For the $Ga_{0.47}In_{0.53}As/Al_{0.24}Ga_{0.23}In_{0.53}As/InP$ system the Q_C between ternary (quaternary) alloy and InP is known with more or less accuracy. It means that the obtained Q_C for $Ga_{0.47}In_{0.53}As/Al_{0.24}Ga_{0.23}In_{0.53}As$ interface can be verified in the context of literature data for this material system.

Figure 5 shows the band gap discontinuities for the $Ga_{0.47}In_{0.53}As/Al_{0.24}Ga_{0.23}In_{0.53}As/InP$ system. After Ref. 39 it has been assumed that the Q_C for $Ga_{0.47}In_{0.53}As/InP$ interface is 40%. This value is well known for this system and is generally accepted. Taking into account the obtained result that the Q_C for the $Ga_{0.47}In_{0.53}As/Al_{0.24}Ga_{0.23}In_{0.53}As$ interface equals 60% and assuming that the Q_C for the $Ga_{0.47}In_{0.53}As/InP$ interface is 40% [39] it has been found that the Q_C for the $Al_{0.24}Ga_{0.23}In_{0.53}As/InP$ interface is smaller than 13% (if the Q_C for the $Ga_{0.47}In_{0.53}As/InP$ is equal 35% then the Q_C for the $Al_{0.24}Ga_{0.23}In_{0.53}As/InP$ interface is smaller than 2%). The obtained values of Q_C for the $Al_{0.24}Ga_{0.23}In_{0.53}As/InP$ interface are consistent with the literature data since it has been reported that the conduction band line-up for this system changes from type I to type II at the Al concentration of ~22–26% [40,41].

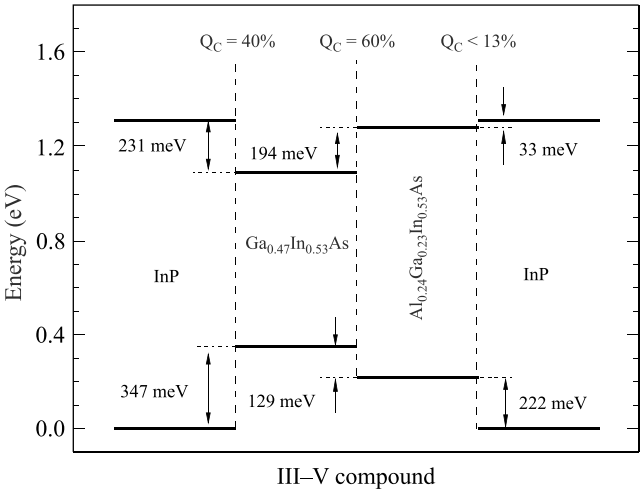

Fig. 5. Band gap alignment for $InP/Ga_{0.47}In_{0.53}As/Al_{0.24}Ga_{0.23}In_{0.53}As/InP$ system.

The energy level structure is difficult to predict for QWs containing dilute nitrides because of unusual change in the band structure of III–V host after the incorporation of a few per-cent of nitrogen atoms [43]. Modulation spectroscopy including CER is often employed to study band offset in such QWs [11–14]. In addition, it has been observed that the incorporation of nitrogen atoms into III–V host generates point defects in this material system. These defects want to pin the Fermi-level at the Fermi stabilization energy [15, 42]. It is possible to observe this effect in CER spectroscopy due to its high sensitivity to the built-in electric field which for bulk-like materials is manifested by FKO [7].

Figure 6 shows CER spectra measured at room temperature for $Ga_{0.78}In_{0.28}N_xAs_{1-x}$/GaAs QW structures of various nitrogen concentrations. In addition to the strong GaAs--related signal at 1.42 eV, CER resonances related to optical transitions in QW region are clearly visible. These transitions shift to red with the increase in nitrogen concentration due to the N-related reduction of energy gap for GaInNAs alloys [44]. The analysis of energies of QW transitions allows us to determine the Q_C at the GaInNAs/GaAs interface. Using this approach it has been reported that the Q_C for GaInNAs/GaAs QW with a few per-cent of nitrogen and ~30–40% of indium atoms is close to 80% [13,14,44]. Very similar Q_C has been found for QW structures shown in Fig. 6. In addition, it is observed that the period of FKO changes due to nitrogen incorporation. This observation is associated with the tendency of the Fermi-level shift to a given energy in the GaInNAs QW region due to N-related defects [15,42]. It has been observed that this energy is close to the Fermi-level stabilization energy which is located ~4.9 eV below the vacuum level [45]. This effect is illustrated in Fig. 7, where the band bending is plotted for N-free and N-containing QWs. In the case of GaInAs/GaAs QW, a pinning of the Fermi-level is expected at GaAs surface and GaAs(buffer)/GaAs(substrate) interface only. It means that more or less homogeneous distribution of a built-in electric field is expected in GaAs barriers. For N-containing QWs the distribution of the built-in electric field is changing since the N-related point defects in QW area want to pin the Fermi-level close to Fermi-stabilization energy [15,42].

For laser applications the active part is very often a step--like barrier (SLB) QW since the proper tuning of quantum barriers can improve laser performances. For such a structure it is interesting to investigate the number of confined states as well as energies of step-like barriers. CER spectroscopy due to its absorption-like character is an excellent tool to study such issues [46,47].

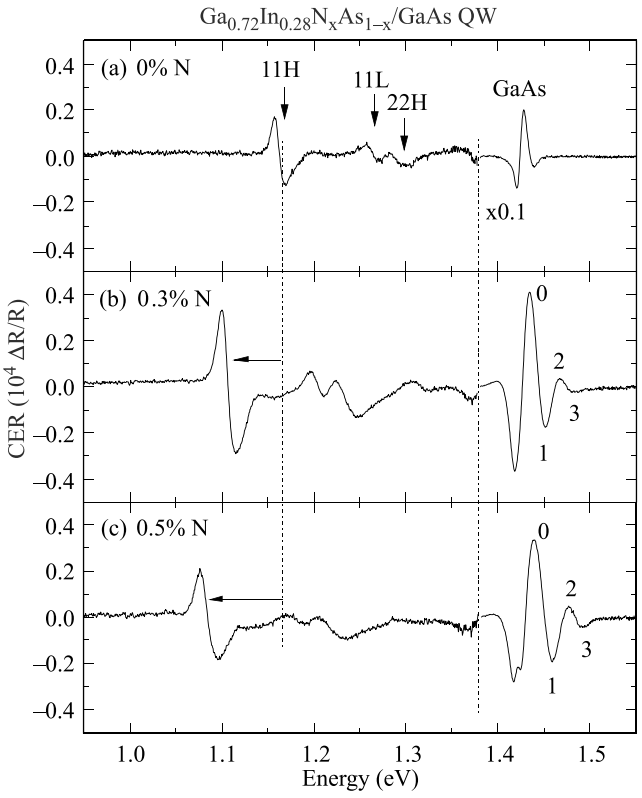

Fig. 6. Room temperature contactless electroreflectance spectra of $Ga_{0.78}In_{0.28}N_xAs_{1-x}$/GaAs QW structures with various nitrogen concentrations.

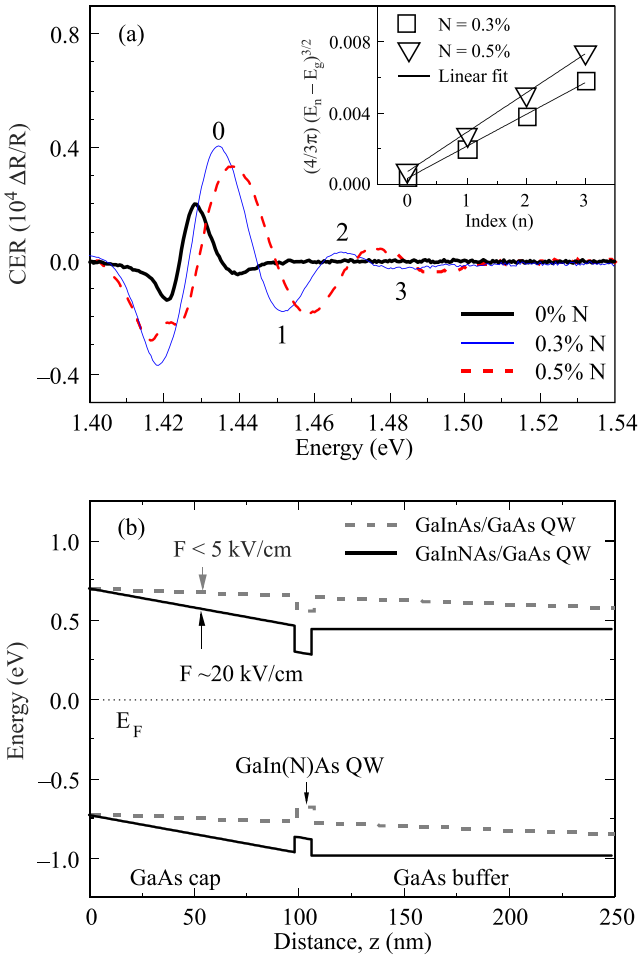

Fig. 7. Room temperature contactless electroreflectance spectra of $Ga_{0.78}In_{0.28}N_xAs_{1-x}$/GaAs QW structures in the vicinity of GaAs transition (a); analysis of GaAs-related Franz-Keldysh oscillations, inset in panel (a); band bending for GaInAs/GaAs (dashed grey lines) and GaInNAs/GaAs (solid black lines) QW structures (b).

Figure 8 shows room temperature CER spectra of a GaInNAs/GaInNAs/GaAs SLB double QW structure, see layer contents in the figure caption and Ref. 47. Besides the strongest part of CER signal at 1.42 eV, which is related to GaAs barriers, two portions of CER signal have been identified for this structure.

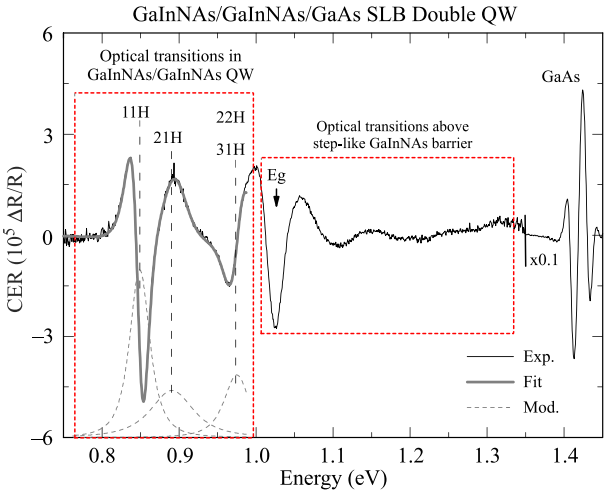

Fig. 8. Room temperature contactless electroreflectance spectra of $Ga_{0.62}In_{0.38}N_{0.02}As_{0.98}/Ga_{0.97}In_{0.03}N_{0.02}As_{0.98}$/GaAs SLB double QW structure.

The first portion between ~0.8 eV and ~1.0 eV is associated with the optical transitions in the active part of the structure, i.e., the GaInNAs/GaInNAs QW. This part is fitted by three resonances which have been identified on the basis of theoretical calculations as the 11H, 21H and 22H/31H transitions [47]. The calculated energy level structure for this QW is shown in Fig. 9(a). It is worth noting that the symmetric and asymmetric state for this double QW is considered as one state twice degenerated since the energy splitting between these states is very small. Optical transitions related to light holes are not considered in this case since the analysed GaInNAs/GaInNAs QW is type II for light holes. However such transitions can be expected above the energy of SLB (i.e., >1.0 eV). Regarding the GaInNAs QW transition the second resonance (21H transition) is observed ~38 meV above the 11H resonance, which is the fundamental transition for this system. It is worth noting that this transition is observed for this QW structure due to: i) some imperfections in the shape of the QW potential, ii) finite QW barriers, and iii) a built-in electric field in this structure. Because of these factors the selection rules typical of square-like QWs are not appropriate for this structure. The third resonance in Fig. 8 at ~0.97 eV could be related to both a transition between the third heavy-hole and the first electron subbands (31H) and a transition between the second heavy-hole and the second electron subbands (22H). According to theoretical calculations for this system the 31H and 22H transitions are expected ~87 and ~114 meV above the fundamental transition, respectively. It is very

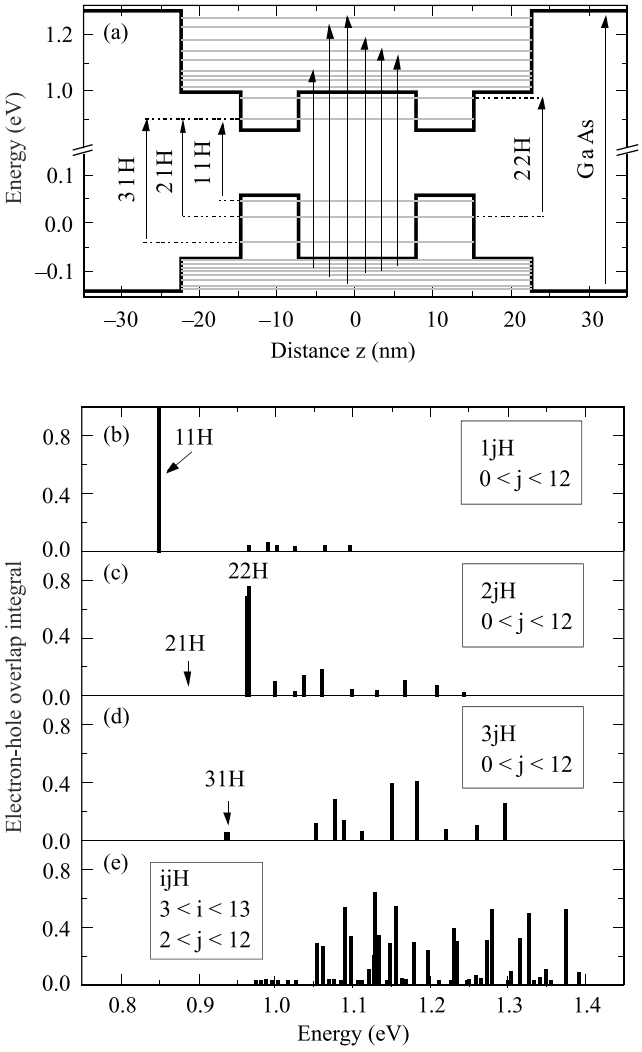

Fig. 9. Energy levels for $Ga_{0.62}In_{0.38}N_{0.02}As_{0.98}/Ga_{0.97}In_{0.03}N_{0.02}As_{0.98}$/GaAs SLB double QW structure (a) and electron-hole overlap integrals for optical transitions in this structure (b) – (e).

close and, therefore, CER resonances related to the two transitions are not resolved in CER spectrum. Moreover, it is worth noting that the oscillator strength related to the 31H transition is weaker than this one associated with the 22H transition.

The second portion of CER signal between ~1.0 and ~1.4 eV (see Fig. 8) is related to optical transitions above the SLB barrier. It is worth noting that this signal is similar to FKOs, however such an oscillation is rather not expected for this structure. Moreover, the analysis of this signal in the scale typical of FKO behaviour shows a non-linear dependence which confirms non FKO origin of this signal. Therefore, the part of CER spectrum between ~1.0 and ~1.4 eV has been attributed to *ij*H transitions in the GaInNAs/GaInNAs/GaAs SLB double QW structure, where $i > 3$ and $j > 2$. At least nine confined states for both electrons and heavy-holes have been found above the SLB in theoretical calculations. It leads to many optical transitions with non-zero oscillator strengths. The electron-hole overlap which

corresponds to the oscillator strength has been calculated for this structure and diagrams of intensities of optical transitions *vs.* the transition energy have been built and plotted in Fig. 9(b)–(e). Panels (b), (c), and (d) show the electron-hole overlap for 1*j*H, 2*j*H, and 3*j*H transitions with $0 < j < 12$, respectively. Electron-hole overlaps for optical transitions between hole and electron levels confined above the SLB are shown in Fig. 9(e). The strongest oscillator strength is observed for 11H and 22H transitions while the oscillator strength for 21H and 31H transitions is much smaller. The oscillator strength for 21H and 31H transitions increases if some imperfections of the symmetry of the QW shape are taken into account. Simultaneously, these imperfections lead to a decrease of the oscillator strength for 11H and 22H transitions. Also, a non-zero electron-hole overlap is observed for 1*j*H, 2*j*H, and 3*j*H transitions with $2 < j < 12$. For some of them the oscillator strength is quite strong (the electron-hole overlap is ~0.4). Also very strong oscillator strength is observed for optical transitions between hole and electron levels confined above the SLB, see Fig. 9(e). A change in the symmetry of the SLB double QW potential leads to some changes in the transition intensities, i.e., the electron-hole overlap for some transitions increases and for other transitions decreases. However, the diagram of the electron-hole overlap is more or less similar to this one shown in Fig. 9(e). It means that spectral features observed in CER spectrum between ~1.0 and ~1.4 eV are related to optical transitions between hole and electron levels confined above the SLB. Such a CER signal is a superposition of many optical transitions separated by small energies as it is shown in Fig. 9. CER resonances related to these transitions can interfere constructively and/or destructively because they have different shapes. The strongest CER signal in this spectral range can be attributed to the energy gap of SLB.

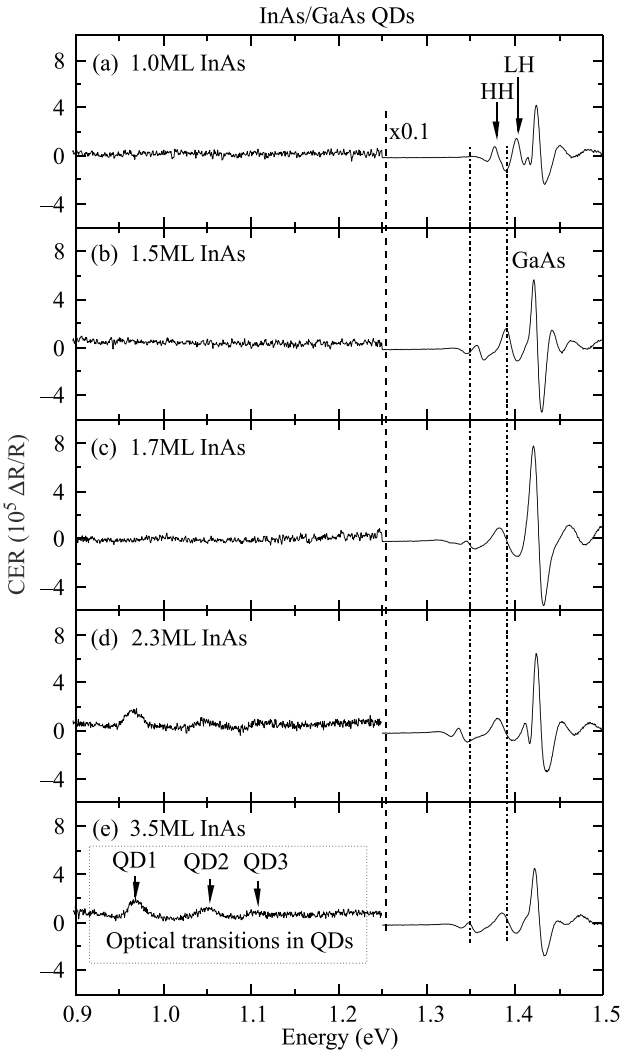

Fig. 10. Room temperature contactless electroreflectance spectra of InAs/GaAs QD samples of various amounts of deposited InAs material.

3.3. Quantum dots and dashes

Quantum dots (QDs) usually contain more than one confined state for electrons and holes. Optical transitions between these states can be probed by PL despite the emission-like character of this technique. It is possible because of small volume of QDs and their low density in comparison to photon density used in standard PL measurements. It is worth noting that the same photon density applied to PL measurements of a QW allows to detect the fundamental transition only because of larger volume of QW in comparison to the QD volume and faster carrier thermalization and recombination. CER spectroscopy due to their high sensitivity and absorption-like character is able to probe the each allowed optical transition in QDs as well as optical transitions in the wetting layer [48–50]. A few examples of the application of CER spectroscopy to study QD structures is presented below.

Figure 10 shows room temperature CER spectra measured for a set of QD samples with various amount of InAs deposited on GaAs substrate [51]. For the InAs/GaAs QD system a formation of InAs QDs appears when the amount of deposited InAs is larger than 1.6 mono-layers (MLs). Below this thickness the whole InAs material is used to formation of a wetting layer, i.e., a very thin QW. Such a QW confines one state for electrons, heavy-holes, and light--holes. Optical transitions between these states are observed in CER spectra. The HH and LH resonances in Fig. 10 are related to optical transitions between the heavy- and light--hole subband and the electron subband, respectively. These resonances shift to red when the InAs amount increases from 1.0 to 1.5 MLs since the width of the thin QW increases as well. With the further increase of the InAs amount the width of wetting layer QW does not increase since the deposited material is used to InAs QD formation. In Fig. 10 it is clearly visible that for samples with InAs > 1.5 MLs the HH and LH transitions do not shift to red within experimental error and some CER resonances appear below the energy of HH transition. This signal is associated with photon absorption in InAs QDs. It is worth noting that the intensity of optical transitions observed in absorp-

tion-like experiment is proportional to the volume of absorbing material. This volume is very small for InAs QDs but it is possible to probe these transitions in CER spectroscopy due to its differential character and very high sensitivity, see in Fig. 10 that the detected CER signal is the order of 10^{-5} $\Delta R/R$.

When an InAs layer is deposited on an InP substrate both regular QDs and elongated QDs (so called quantum dashes) can be formed depending on the growth conditions [52]. For both QDs and quantum dashes (QDashes) a wetting layer is formed but the quantum confinement for electrons is much weaker for InAs/InP system than for InAs/GaAs one due to a smaller conduction band offset at the InAs/InP interface. Because of this feature, optical transitions in the InAs/InP wetting layer QW are very sensitive to built-in electric field (e.g., a surface electric field). This field can significantly change the electron-hole overlap for HH and LH transitions and, therefore, spectral features related to these transitions can be sometimes not observed for InAs QDs and/or QDsashes grown on InP substrate.

Figure 11 shows an example of application of CER spectroscopy to study optical transitions in InAs/InP QD samples obtained at various growth conditions. For the three samples a strong PL signal from InAs QDs is observed at ~0.7–1.1 eV. CER signal related to photon absorption in InAs QDs is also observed in this spectral range. The strongest CER signal is observed for the three samples at the energy of ~1.35 eV. This resonance is associated with the photon absorption in InP cap/buffer layer. CER resonances related to the photon absorption in InAs wetting layer are clearly visible only for the sample # 1. For samples # 2 and # 3 the electron confinement in the wetting layer region probably is much weaker and, therefore, HH and LH transitions are not observed for the two samples. It is worth noting that weaker quantum confinement for electrons in some InAs/InP QD samples can result from different band bending around InAs QD layer. Very similar situation is also expected for InAs QDash structures. However, spectral features related to photon absorption in InAs wetting layer have been observed in CER spectra [50].

Figure 12 shows room temperature CER and PL spectra of an InAs QDash structure, see details of this structure in Ref. 50. CER signal related to photon absorption in InAs QDashes is observed at the energy of ~0.75 eV. This signal is very well correlated with the PL signal. A weak resonance associated with the photon absorption in InAs wetting layer is also observed in this spectrum, see the spectral feature at the energy of ~0.9 eV. The strongest CER resonance in this spectrum is related to the photon absorption in AlGaInAs barriers. For the InP capped structure a CER resonance

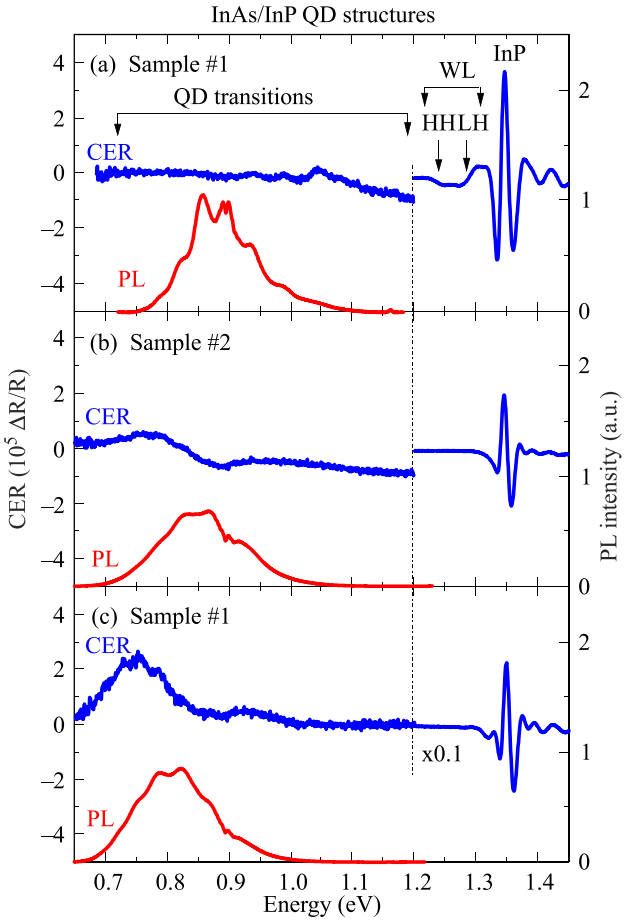

Fig. 11. Room temperature contactless electroreflectance (blue curves) and photoluminescence (red curves) spectra of InAs/InP QD samples obtained at various growth conditions.

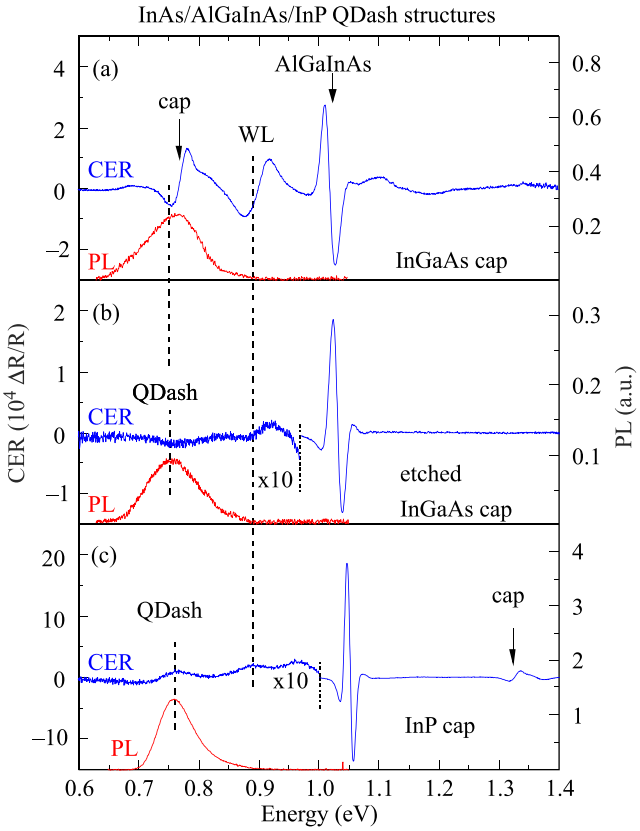

Fig. 12. Room temperature contactless electroreflectance (blue curves) and photoluminescence (red curves) spectra of InAs/InP QDash samples with various cap layers.

associated with the photon absorption in InP cap layer is also observed at the energy of ~1.35 eV.

3.4. Quantum dots and dashes embedded in a quantum well

For QDs embedded in a QW it is possible to probe optical transitions in QDs as well as optical transitions in the surrounded QW [53,54]. It means that the band structure of the surrounded QW can be determined from CER measurements. In general, the surrounded QW helps to tune the QD emission but this QW also influence laser performances and, therefore, it is important to know the band structure of both QDs and the surrounded QW.

Figure 13 shows CER and PL spectra measured for In(N)As QDs embedded in GaIn(N)As QW [54]. First it is visible that the QD emission redshifts due to the incorporation of N atoms into the InAs/GaInAs system. A redshift of CER resonance, which is related to QD absorption, is also observed in these spectra. The strongest CER signal, which is observed at ~1.42 eV, is associated with bulk-like absorption in GaAs barriers. In addition to the GaAs transition and QD transitions, CER resonances, which are associated with optical transitions in the In(N)As/GaIn(N)As/GaAs QW, are clearly visible in CER spectra (see CER resonances between ~1.15 and 1.4 eV). It is worth noting that the optical transitions in the surrounded QW are not observed in PL spectra whereas QD transitions (both the ground and excited state ones) are visible in PL spectra. Therefore, the most interesting part of CER spectrum, in this case, is the one which is associated with the optical transitions in the In(N)As/GaIn(N)As/GaAs QW. A knowledge of the number of confined states in the surrounded QW and their energies is important from the point of view of such processes as i) the thermal quenching of QD emission and ii) the carrier relaxation to the ground state in QDs.

In order to extract energies of the QW transitions, CER spectra in the range of QW transitions have been fitted by Eq. (3) with $m = 3$. Fitting curves and modulus of CER resonances are plotted in Fig. 13. The identification of the resonances is possible on the basis of the calculations performed in the framework of the effective mass approximation, see details in Ref. 54. As in the previous case, the notation *kl*H(L) in Fig. 13 denotes the transition between the *k*-th heavy-hole (light-hole) valence subband and the *l*-th conduction subband. In addition to the fundamental QW transition (11H), CER spectra show an 11L transition (i.e., the fundamental transition for light-holes) and transitions between excited QW states (21H and 31H). Note that the selection rules for a square-like QW do not work for this QW due to strong asymmetry of QW potential in this system.

The calculated band structure and wave-functions for In(N)As/GaIn(N)As/GaAs QWs can be found in Ref. 54. It has been found that the QWs confine one electron, one light-hole and three heavy-hole states. The energy separation between the QD and QW ground state transitions in this system has been found to be ~250 meV. Taking into account

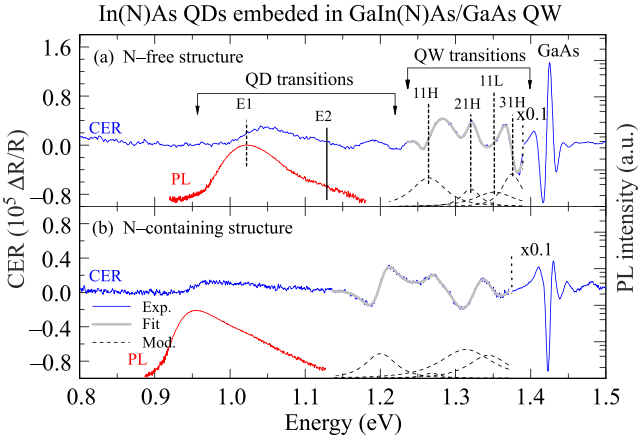

Fig. 13. Room temperature contactless electroreflectance (blue curves) and photoluminescence (red curves) spectra of InAs/GaInAs/GaAs (a) and InNAs/GaInNAs/GaAs (b) QD structures.

this fact that QD excited state transitions are observed in CER spectra, it can be concluded that this system has the energy separation between electron (heavy-hole) QD and QW ground states much higher than the thermal energy at room temperature. It means that this design of gain medium is very perspective for laser applications.

Figure 14 shows PL and CER spectra measured for InAs QDashes embedded in $Ga_{0.47}In_{0.53}As/Al_{0.24}Ga_{0.23}In_{0.53}As$ QW. In this set of samples the thickness of InAs layer is changing from 0.8 to 1.3 nm whereas the thickness of the two surrounding $Ga_{0.47}In_{0.53}As$ layers is constant and equals 5 nm. It means that the InAs layer is inserted centrally inside the 10-nm wide $Ga_{0.47}In_{0.53}As/Al_{0.24}Ga_{0.23}In_{0.53}As$ QW. Such a QW system is discussed in Sect. 3.1 and the Q_C at the $Ga_{0.47}In_{0.53}As/Al_{0.24}Ga_{0.23}In_{0.53}As$ interface has been determined to be Q_C~60%, see Figs. 4 and 5. In this case it is interesting to investigate how the InAs layer influences the energy level structure in this QW and what is the nature of emission peak for these structures.

In PL spectrum in Fig. 14 only one peak is observed. This peak shifts from 0.71 to 0.64 eV with the increase in InAs thickness from 0.8 to 1.3 nm. It is expected that this PL corresponds to the recombination between the ground electron state and the ground heavy-hole state of entire InAs/$Ga_{0.47}In_{0.53}As/Al_{0.24}Ga_{0.23}In_{0.53}As$ system. Since the band gap discontinuity for InAs/$Ga_{0.47}In_{0.53}As$ interface is generally considered to be of Type I for both electrons and holes, it can be assumed that InAs/$Ga_{0.47}In_{0.53}As$ QDashes have at least one confined state for electrons and heavy-holes and the emission peak is related to the recombination between these states. It is necessary to note that the observed peak is asymmetric. Its high energy shoulder may be the evidence of the existence of the $\boldsymbol{k}$ vector in QDash structures, since the quantization in one direction (dash length) is negligible because the energy difference between levels is smaller than thermal energy (i.e., kT). On the other hand such an asymmetric PL peak is typical for QW system at room temperature (due to the same reason). Therefore, on

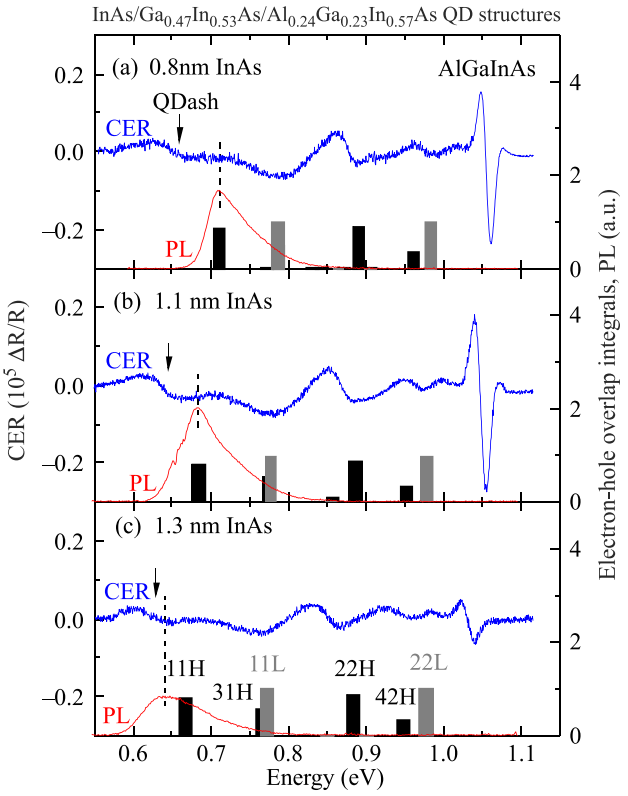

Fig. 14. Room temperature contactless electroreflectance (blue curves) and photoluminescence (red curves) spectra of InAs/$Ga_{0.47}In_{0.53}As/Al_{0.24}Ga_{0.23}In_{0.53}As$ QDash structures with various amounts of InAs material.

the basis of PL only, it is not possible to exclude that at least one of the states involved in the recombination process is confined in $InAs/Ga_{0.47}In_{0.53}As/Al_{0.24}Ga_{0.23}In_{0.53}As$ QW potential, i.e., the $InAs/Ga_{0.47}In_{0.53}As$ system is of Type-II and optical transition occurs between a quasi-three-dimensionally confined state of the dash potential and a state confined in one dimension of the QW only. More reliable conclusions on the energy structure in this system can be extracted from CER data which contain information about energies of excited states as well as the energy of the QW barrier.

In case of the CER spectrum shown in Fig. 14, as many as five characteristic PR features can be resolved below the resonance at 1.052 eV originating from $Al_{0.24}Ga_{0.23}In_{0.53}As$ barrier layer [55]. The identification of the resonances is possible on the basis of the calculations performed in the framework of the effective mass approximation. In the first approximation, in order to estimate the number of optical transitions in $InAs/Ga_{0.47}In_{0.53}As/Al_{0.24}Ga_{0.23}In_{0.53}As$ system as well as their energies, the InAs layer can be omitted and the optical transitions in a single 11-nm thick $Ga_{0.47}In_{0.53}As/Al_{0.24}Ga_{0.23}In_{0.53}As$ QW can be calculated. In the next step the energy levels of the whole $InAs/Ga_{0.47}In_{0.53}As/Al_{0.24}Ga_{0.23}In_{0.53}As$ system can be calculated, taking into account no formation of QDashes in the InAs layer (as a kind of an approximation again). The InAs layer is assumed to be coherently strained and to have the nominal thickness of InAs layer, i.e., 0.8, 1.1, and 1.3 nm. In general, the formation of thin InAs WL is expected for this system, but the thickness of the WL is smaller than the nominal InAs layer thickness similarly as in QD structures. Calculations have been carried out assuming that the Q_C for $InAs/Al_{0.24}Ga_{0.23}In_{0.53}As$ and $Ga_{0.47}In_{0.53}As/Al_{0.24}Ga_{0.23}In_{0.53}As$ interface is 70% [50] and 60%, respectively [38].

Figure 15 shows energy levels and possible optical transitions for the structure with 1.1-nm thick InAs layer. In addition, integrals of electron-hole overlap for optical transitions in these structures are plotted in Fig. 14, see black and grey bars; as for previous examples the notation *kl*H(L) denotes the transition between *k*-th heavy-hole (light-hole) valence subband and *l*-th electron conduction subband. Basing on the energy band structure shown in Fig. 15, it becomes easier to explain such a high broadening of some resonances and the nature of PL peak. Due to significant fluctuations of the "effective" InAs layer thickness related to QDash formation the broadening of the first electron and heavy-hole levels is much larger than the broadening of the energy levels confined above the intermediate $Ga_{0.47}In_{0.53}As$ barrier, i.e. the energy levels confined in a regular QW with

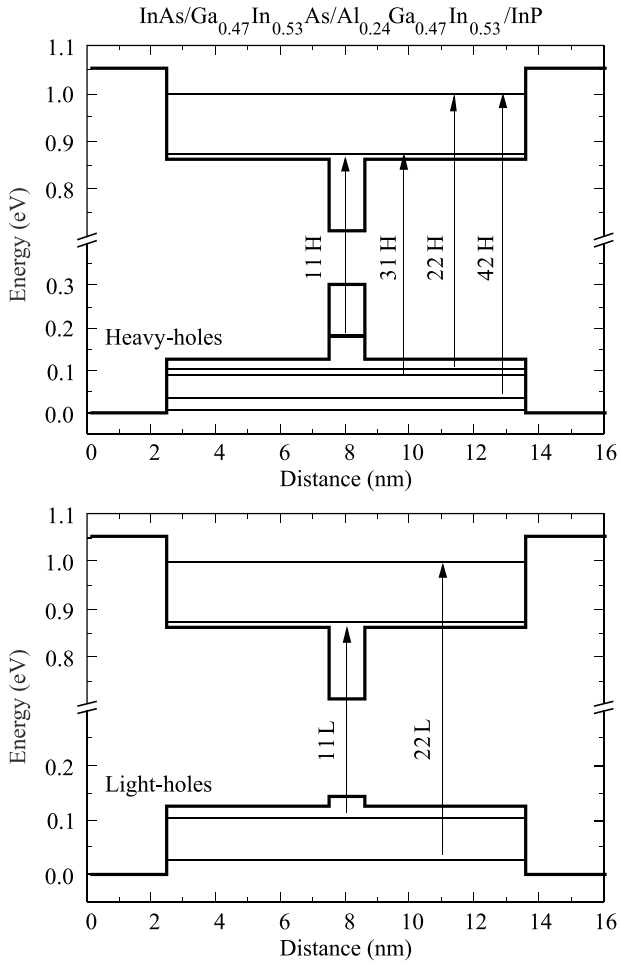

Fig. 15. Energy levels calculated for $InAs/Ga_{0.47}In_{0.53}As/Al_{0.24}Ga_{0.23}In_{0.53}As$ QDash structure with marked optical transitions for which electron-hole overlap integral is significantly larger than zero.

low roughness interfaces. For example see CER resonances at ~0.87 and ~0.97 eV and compare them with the CER resonance at ~0.75 eV.

It is worth noting that an additional CER feature is observed below the calculated ground state transition in the whole InAs/$Ga_{0.47}In_{0.53}As$/$Al_{0.24}Ga_{0.23}In_{0.53}As$ system, see arrows in Fig. 14. This feature is connected with the fundamental transition in QDashes. For the structure with the thinnest InAs layer this feature does not correlate with PL peak but this correlation improves with the increase in InAs thickness. It is worth noting that a very nice correlation between the QDash resonance and PL peak is observed at low temperatures (not shown here) that confirms that QDashes are the main recombination channel in these structures at low temperatures. However, the energy separation between the QDash transition and the QW ground state transition is too small to prevent QDash excitons from the thermal quenching at room temperature. Therefore the room temperature PL is a superposition of QDash and QW emission. The contribution QW emission is the strongest for structures with the thinnest InAs layer and this contribution decreases with the increase in InAs thickness and the temperature decrease.

3.5. Quantum dots/dashes coupled with a quantum well

The discrete density of states for QDs and QDashes makes possible the low-threshold current laser operation, however, at the same time it also restricts the fast phonon-assisted relaxation mechanism from the excited to the ground state by reducing the efficiency of lasing and preventing ultra--high-frequency modulation. Recently QDash based lasers employing an auxiliary QW placed near the QDash layer and separated by a thin barrier have been developed [56]. This arrangement provides much faster carrier injection into QDashes and solves the problem with carrier relaxation due to the carrier tunnelling from a QW to QDashes through a thin quantum barrier. The carrier injection efficiency in the "so called" tunnel-injection (T-I) structures depends on many factors [56–58] including the energy levels in the auxiliary QW and the quasi-0 dimensional (0D) objects. In addition, the existence of the layer of self-assembled QDashes affects the energy states in the neighbouring QW which is separated by the thick barrier layer [57]. CER spectroscopy is a good tool to study the band structure of such T-I structures [57].

Figures 16(a), 16(b), and 16(c) show room temperature CER spectra of the two reference samples ($Ga_{0.47}In_{0.53}As$/$Al_{0.24}Ga_{0.23}In_{0.53}As$ QW and InAs QDash samples which are also shown in Figs. 3 and 12, respectively) and the T-I structure with the 3-nm thick barrier, respectively. There is worth noting that the strongest CER signal is observed for the three samples at ~1.06 eV and this resonance is associated with the photon absorption in a bulk-like $Al_{0.24}Ga_{0.23}In_{0.53}As$ layer which is a quantum barrier for InAs QDashes

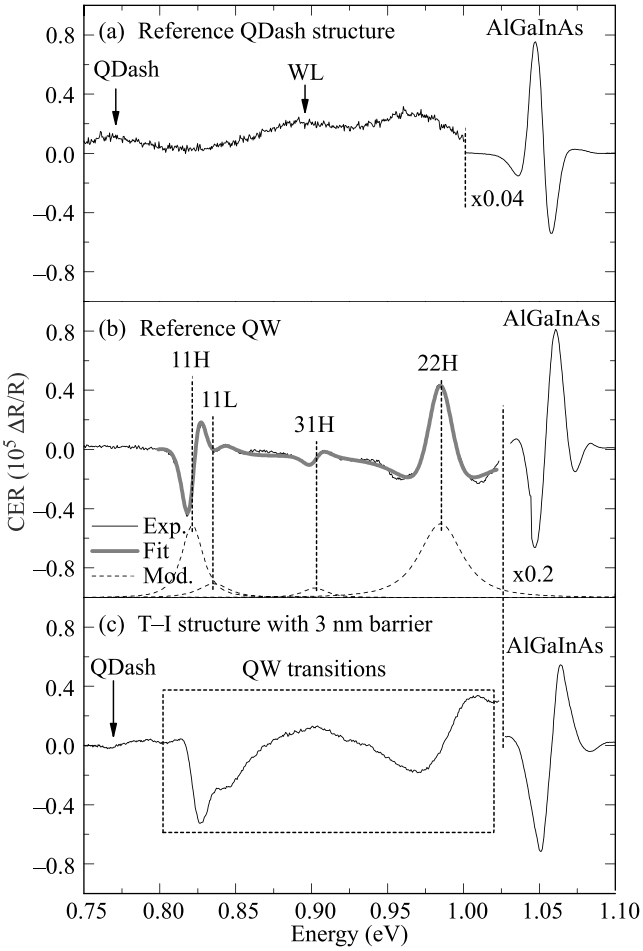

Fig. 16. Room temperature contactless electroreflectance spectra of reference InAs/InP QDash (a) and $Ga_{0.47}In_{0.53}As$/$Al_{0.24}Ga_{0.23}In_{0.53}As$ QW (b) samples and the T-I structure ($Ga_{0.47}In_{0.53}As$--InAs) with 3 nm barrier (c).

and $Ga_{0.47}In_{0.53}As$ QW. Below that, CER features related to optical transitions in InAs QDashes and $Ga_{0.47}In_{0.53}As$ QW are expected. Spectral features observed for reference samples have been identified in previous figures (Figs. 3 and 12) as the optical transitions in $Ga_{0.47}In_{0.53}As$/$Al_{0.24}Ga_{0.23}In_{0.53}$ As QW and InAs QDashes and InAs wetting layer. For the T-I structure the CER spectrum appears to differ significantly when compared to the reference samples, see Figs. 16(a), 16(b), and 16(c). It is clearly visible that all transitions are more broadened and a weak CER feature is observed below the energy of ~0.8 eV. The latter one is attributed to the QDash ground state transition whereas all CER features within the dashed box in Fig. 16(c) are related to the light absorption in the QW region composed of $Ga_{0.47}In_{0.53}As$ and InAs layers. It is worth noting that in case of a lack of quantum-mechanical coupling between the states confined inside the $Ga_{0.47}In_{0.53}As$ and InAs potentials, a superposition of independent CER resonances related to both parts should be expected, i.e., the CER spectrum of T-I structure should be a superposition of CER spectrum measured for InAs QDashes and $Ga_{0.47}In_{0.53}As$/$Al_{0.24}Ga_{0.23}In_{0.53}As$ QW.

However, CER spectrum observed for the T-I structure is quite different. This strong change in CER spectrum in the range of QW transitions is an evidence of a strong coupling between the $Ga_{0.47}In_{0.53}As$ and InAs potential wells in sense of significant tunnelling probability through the separating barrier. It is worth noting that an InAs wetting layer is indeed formed during the growth of self-assembled InAs dashes on InP substrate, and it is optically active, see the previous discussion on wetting layer transitions in InAs QDashes grown on InP and Refs. 50 and 59. Its thickness has been estimated to be about 0.7–1 nm, whereas the conduction band offset for the $InAs/Al_{0.24}Ga_{0.23}In_{0.53}As$ interface is close to 70% [50]. In case of the T-I structures, it is expected that the addition of the potential associated with the InAs WL affects the energies and wave-functions of electrons and holes confined in the QW. It means that the T-I structure should be considered as a system with the QW confinement potential composed of $Ga_{0.47}In_{0.53}As/Al_{0.24}Ga_{0.23}In_{0.53}As$ QW and the $InAs/Al_{0.24}Ga_{0.23}In_{0.53}As$ WL QW, i.e., an asymmetric double quantum well.

In order to explain the spectral features observed for the T-I structure in Fig. 16(c), energy level calculations have been performed for the system composed of both the $Ga_{0.47}In_{0.53}As$ and InAs potentials. It has been assumed that the conduction band offset for $Ga_{0.47}In_{0.53}As/Al_{0.24}Ga_{0.23}In_{0.53}As$ and $InAs/Ga_{0.47}In_{0.53}As/Al_{0.24}Ga_{0.23}In_{0.53}As$ interface is 60% and 70%, respectively, and the WL thickness is 1.0 nm [38,50]. For calculations of the QW-like states the QDash-related potential is neglected. The obtained energy levels and wave-functions for the T-I structure with a 3-nm barrier are shown in Fig. 17. It is clearly visible that the probability that an electron (or a hole) is localized on the side of the GaInAs or InAs layer, varies with the energy level. Moreover, it is visible that the selection rules typical for the square-like QWs cannot be employed for the T-I system, i.e., the system composed of $Ga_{0.47}In_{0.53}As/Al_{0.24}Ga_{0.23}In_{0.53}As$ and InAs QWs. It means that all the possible optical transitions have to be considered for T-I structures and optical transitions with non-zero electron-hole wave-function overlap should be taken into account in CER spectra.

Figures 18(a), 18(b) and 18(c) show the room temperature CER spectra together with the calculated electron-hole overlap integrals for the T-I samples with 4-, 3-, and 2-nm barriers, respectively. These calculations confirm that the CER signal observed below the energy of 0.8 eV is associated with the optical transition in QDashes whereas the remaining CER features can be related to the appropriate optical transitions between the hole and electron levels in the GaInAs-InAs QW system. The latter optical transitions are separated by a small energy compared to the line broadening and therefore, they are not fully resolved in the CER spectra. However, the three spectra strongly confirm the

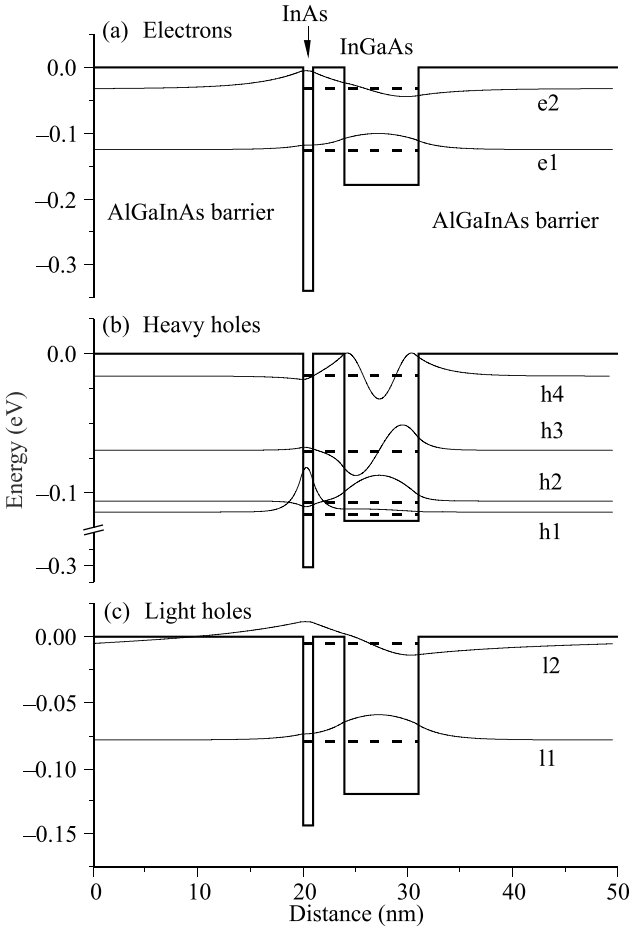

Fig. 17. Energy levels and wavefunctions for the T-I structure ($Ga_{0.47}In_{0.53}As$-InAs) with 3-nm barrier.

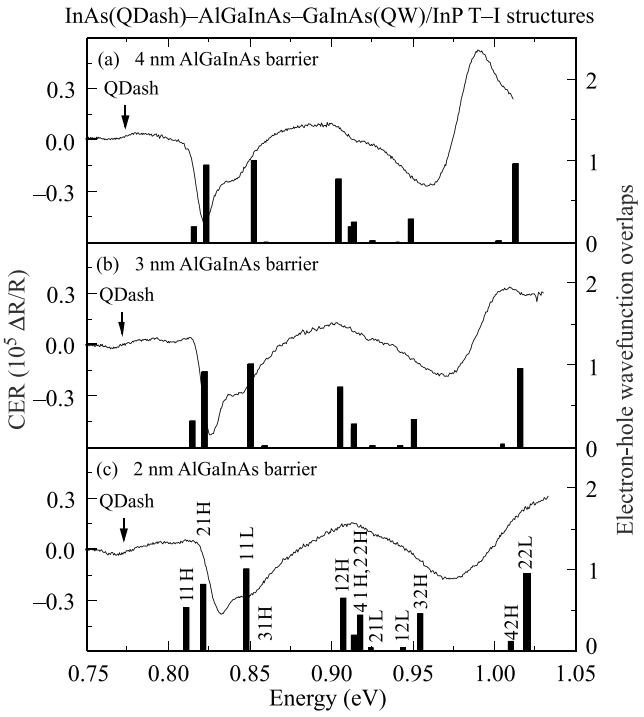

Fig. 18. Room temperature contactless electroreflectance spectra of the T-I structure ($Ga_{0.47}In_{0.53}As$-InAs) with 4-nm (a), 3-nm (b), and 2-nm (c) barrier and theoretical calculations of electron-hole overlap integrals for these structures.

character of the confinement potential for electrons (holes) in the growth direction. It means that there are states which are localized in both the $Ga_{0.47}In_{0.53}As$ and InAs layers, respectively. For such a system carriers captured by the $Ga_{0.47}In_{0.53}As$-InAs QW can easily penetrate the QDash region and further can be captured by QDashes and it is expected further that the efficiency of this carrier capturing by particular QDashes should depend on the position of QDash energy levels. This result clearly shows that the energy level structure for QDashes and QWs separated by a thin barrier cannot be considered independently. For such a system a common potential exist for electrons and holes and energy levels for such a potential should be calculated.

4. Contactless electroreflectance *vs*. photo--reflectance

In general, CER spectra are very similar to PR ones because of the modulation of the same parameter, i.e., the modulation of the built-in electric field. However, it is well known that the mechanism of electro-modulation is different for the two techniques. Thus, significant differences between CER and PR spectra can appear for some samples [60–62].

As it is mentioned in Sect. 2 the front electrode in CER measurements, which is semi-transparent for light, is separated from the sample surface by a spacer and, thus, there is nothing with a direct contact with the sample. It means that the sample does not conduct any currents and the external electric field is able to change only the carriers distribution inside the sample. This carriers which are captured by surface states change the surface band bending and lead to a periodic modulation of the surface electric field.

In case of PR, the modulation is caused by photo-excited electron-hole pairs created by the pump source (usually a laser) [1–4]. Photon energy of the pump beam is usually larger than the band gap of the semiconductor being under study. However, there is a possibility to use a below band gap modulation through the excitation of impurity or surface states [63,64]. In both cases photo-generated carriers can be trapped by surface states and in this way the surface band bending is modulated [1–4]. However, it is worth noting here that a lot of interfaces appear inside low dimensional semiconductor structures. In some cases carriers photo-generated in layers separated from the sample surface by another layer cannot move to the surface and hence these carriers cannot change the occupation of surface states, i.e., the surface electric field. However, these carriers effectively change band bending at interfaces inside the sample. It means that the amplitude of band bending modulation can be different for each layer of a complex semiconductor heterostructure. For some samples this amplitude can be effectively tuned by the wavelength of the modulation beam since in this way it is possible to change the quantity of photo-generated carriers in a given layer [65]. Such a possibility does not exist in CER spectroscopy. But on the other hand, the photo-generated carriers are the source of PL signal which is difficult to eliminate in a low temperature or even room temperature PR measurements for QW and QD samples. This problem does not exist in CER spectroscopy since any extra carriers are not generated due to the external modulation. The lack of PL signal in CER measurements is one of the most important advantages of CER spectroscopy.

The other very important difference between CER and PR techniques lies in the deepness of band bending modulation which is much shorter for CER spectroscopy. According to the above discussion this difference results from the modulation mechanism taking place in the two techniques. The smaller sample probing is in favour of CER spectroscopy when the signal from the investigated layer interferes with the unwanted signal from the substrate. But on the other hand, the deeper sample probing can be in favour of PR spectroscopy if we are interested in a signal from a layer which is covered by few other layers. Therefore, very often the two techniques can be complementary in the application to study a complex semiconductor heterostructures. In order to illustrate the above mentioned differences in CER and PR techniques, few examples of application of CER and PR spectroscopy to study the same samples are presented below.

Figures 19(a) and 19(b) show the room temperature CER and the PR spectra of the $Ga_{0.64}In_{0.36}N_{0.046}As_{0.954}/GaN_{0.006}As_{0.994}$ multi QW (MQW) sample, respectively. This sample was grown on GaAs substrate by molecular beam epitaxy. Prior to growth of MQW structure a 300-nm

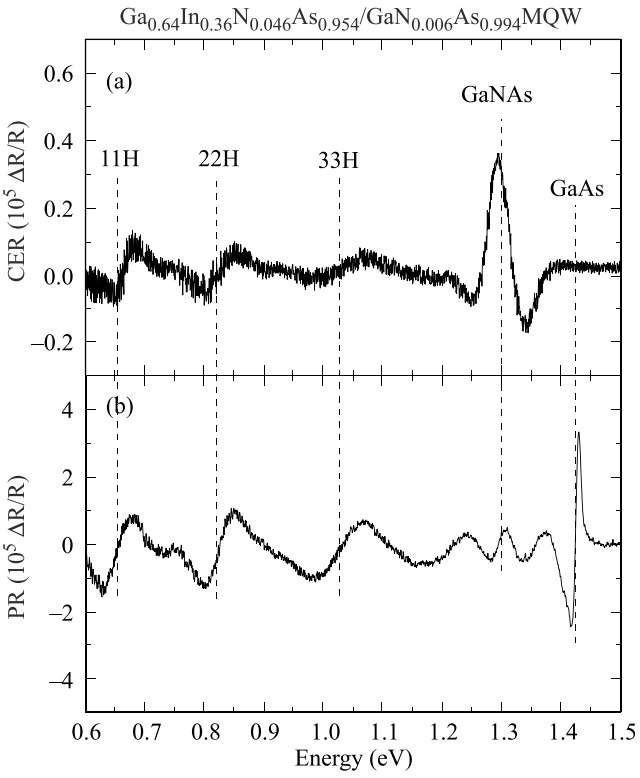

Fig. 19. Room temperature contactless electroreflectance (a) and photoreflectance (b) spectra of $Ga_{0.64}In_{0.36}N_{0.046}As_{0.954}/GaN_{0.006}As_{0.994}$ MQW structure grown on GaAs substrate [13].

thick GaAs buffer layer was deposited directly on GaAs substrate. Next 12-nm thick $GaN_{0.006}As_{0.994}$ and 8.1-nm thick $Ga_{0.64}In_{0.36}N_{0.046}As_{0.954}$ layers were grown and they were repeated ten times. No GaAs cap was deposited on the top of this sample. Other relevant details of the sample growth are described in Ref. 13. The identification of CER resonances was accomplished using standard calculations within the effective mass approximation. As in previous examples the notation *kl*H in this figure denotes the transition between the *k*-th heavy-hole valence subband and the *l*-th conduction subband. For this sample a good agreement between experimental data and theoretical calculations has been obtained assuming that the Q_C for GaInNAs/GaAs interface is 80% and the electron effective mass is 0.09 m_0 [13]. In this case we want to focus on differences between CER and PR spectra measured for the sample. First, it is visible that the GaNAs barrier transition and QW transitions are observed in CER and PR spectra at the same energies within the experimental error. The main difference between CER and PR spectra lies in the signal intensity and the sensitivity to detect the GaAs buffer layer. As is discussed in Ref. 62, a higher amplitude of band bending modulation is easier to achieve in PR spectroscopy. In the case of PR measurements, which are shown in this figure, the intensity of probing beam was 30 mW (at the spot size of ~4 mm^2), i.e., quite strong as for PR spectroscopy. In addition to the band bending modulation at the sample surface, the laser beam (modulating beam) penetrates the GaAs buffer layer, generates electron-hole pairs in this layer and hence modulates band bending at the buffer layer/substrate interface. In the case of CER spectroscopy, the deepness of band bending modulation is very small, because of other modulation mechanism. It means that majority of CER signal originates from the sample area which is close to the surface. Very similar differences in CER and PR spectra were also observed for much simpler structures. For example, it has been shown in Ref. 62 that for uncapped 100-nm thick GaInNAs layers grown on GaAs buffer layer the GaAs--related transition is observed in PR whereas no such a transition is detected in CER spectra. Similar situation is observed in Fig. 19 since the cap layer in this sample is GaNAs layer in fact. The different relative intensities of the GaNAs- and QW-related signal in CER and PR spectra are also associated with different modulation mechanism in these two techniques.

The other effect leading to much smaller deepness of sample probing by CER spectroscopy is the screening phenomenon which is typical of heterostructures with the two--dimensional (2D) electron gas (2DEG) at semiconductor interfaces [66,67]. Figures 20(a) and 20(b) show the PR and CER spectra, respectively, obtained for an AlGaN/GaN heterostructure with a 2DEG at the interface. In the case of PR spectrum, strong PR features are observed at energies corresponding to the GaN and AlGaN band gap. It could be expected that similar features should be observed in CER spectra since the AlGaN layer is very thin ~20 nm. However, any strong GaN-related features are not observed in

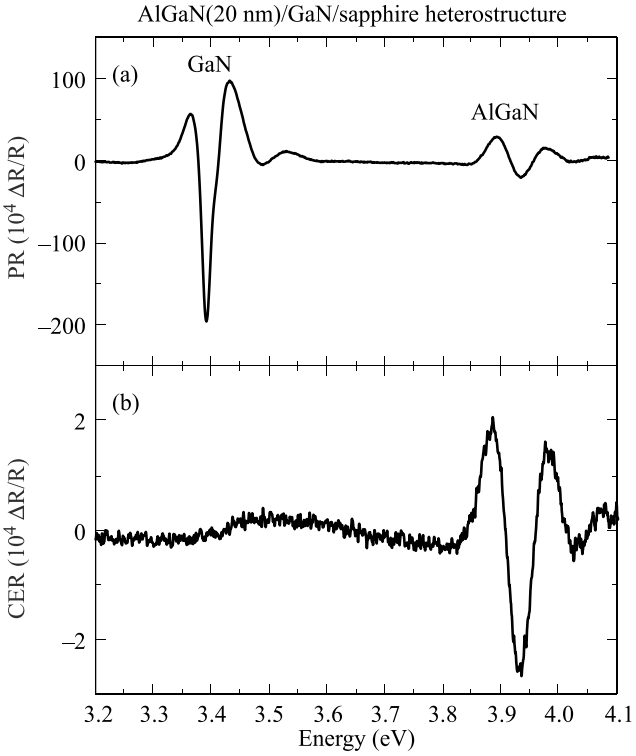

Fig. 20. Room temperature photoreflectance (a) and contactless electroreflectance (b) spectra of AlGaN/GaN heterostructure grown on sapphire substrate.

CER spectra whereas the AlGaN-related signal is still observed. Similar behaviour has been observed for other AlGaN/GaN heterostructures with the 2DEG at the AlGaN/GaN interface. It means that some parts of GaN layer are not probed in CER since the 2DEG at the AlGaN/GaN interface screens the modulation of the built-in electric field in GaN layer [66,67]. In other words, it means that due to the high concentration of 2DEG at AlGaN/GaN interface the external modulation is not able to change band bending in the GaN layer. This phenomenon is often called as screening of the GaN layer in CER spectroscopy by 2DEG [67] and can be used to a quick and contactless detection of 2DEG presence at the AlGaN/GaN interface.

Finally, it is worth noting that for low dimensional structures (QWs, QDs, etc.) an oscillation feature (OF) appear in PR spectra below the energy gap of GaAs if they are grown on n-type GaAs substrates [53,60,68,69]. Sometimes a weak OF is also observed for structures grown on seminsulating GaAs substrates [61]. In general such an OF is an unwanted signal which complicates the analysis of optical transitions in QWs and/or QDs. This OF can be eliminated by applying CER instead of PR. This finding shows that the OF's origin is the modulation of the refractive index in the sample due to the generation of additional carriers by the pump beam (i.e., the laser beam). In the case of CER spectroscopy, any additional carriers are not generated during the modulation hence CER spectra are free of OFs [60,61]. In order to illustrate this advantage of CER spectroscopy

few examples of CER and PR spectra measured for different structures grown on GaAs substrate (n-type and semi-isolating (SI) type) are presented below.

Figure 21 shows a comparison of PR and CER spectra measured at room temperature for InAs/GaAs QDs capped by GaInAs layer. This structure was grown on n-type GaAs substrate and hence the strong OF is observed in PR spectrum below GaAs energy gap. Very similar OF has been observed in PR spectra of other QW and QD structures as well as undoped epilayers grown on n-type GaAs substrates. In general the intensity of OF in such structures is comparable with the intensity of PR signal related to the fundamental transition in GaAs or sometimes this intensity is much stronger than the intensity of GaAs signal. Such a situation complicates the analysis of PR signal associated with QD and/or QW transitions especially that the intensity of such transitions is usually 1–3 magnitudes weaker that the intensity of GaAs transitions. Very often a change in the detection phase helps to eliminate OFs without significant weakness of PR signal related to the optical transitions. However, for some samples OFs' elimination via the selection of an appropriate phase leads to loss of PR signal related to the optical transitions in QDs and/or QWs. Such a situation has been also observed for the sample which is analysed in Fig. 21. Therefore, better approach is to apply CER instead of PR. As it is seen in Fig. 21, spectral features, which could be related to QW transitions, are not well visible in PR spectrum while a lot of sharp resonances is visible in CER spectrum which is free of the OFs. The identification of these resonances is possible on the basis of calculations within the effective mass approximation [11], see details in Ref. 53. As in previous examples the notation *kl*H(L) denotes the transition between *k*-th heavy-hole (light-hole) valence subband and *l*-th conduction subband in the InAs/ GaInAs/GaAs QW potential. The optical transitions in InAs QDs are marked by E1, E2, E3 and E4.

It is worth noting that such an OF is almost always observed for GaAs-based heterostructures grown on n-type GaAs substrates, see for example PR spectra in Refs. 60, 68 and 69. It means that such samples cannot be investigated in detail by PR spectroscopy whereas they can be very carefully investigated by CER spectroscopy. In general, the intensity of OFs for GaAs-based structures grown on n-type GaAs substrate is weaker if the total thickness of the epilayers is higher than one micro-meter. However, no general conclusion about the critical thickness cannot be obtained because the intensity of OFs also depends on other factors such as the content and thickness of the individual epilayers and probably the grown conditions. Such a result confirms that the OFs are related to an interference effect inside the epitaxial layers. The interference effect could be very complex if the sample has lot of epilayers with different refractive indexes. However, the main contribution to OFs originates from the epilayer/substrate interface, because the refractive index has to change differently in the two neighbours layers in order to obtain a signal in PR in the sample transparency region. It is possible if the two layers have different carrier concentrations. Usually the refractive index of epitaxial layers is differently sensitive to the additional carriers than the refractive index of a n-type GaAs substrate. Therefore, an efficient modulation of the difference of refractive indexes could appear during PR measurements where the modulated beam generates additional carriers. The photo-generated carriers are able to change the refractive index. In the case of CER, such a mechanism of the refractive index modulation is absent because in this technique we do not use the laser beam which is the origin of additional carriers.

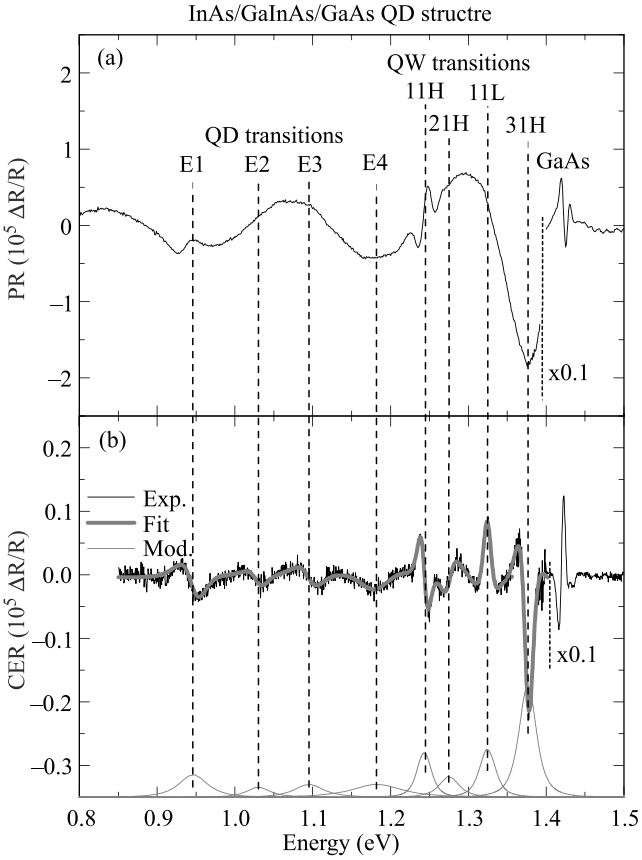

Fig. 21. Room temperature photoreflectance (a) and contactless electroreflectance (b) spectra of InAs QDs capped by 5nm-thick $Ga_{0.85}In_{0.15}As$ layer.

The effective modulation of the refractive index is difficult to obtain if the refractive index in the two neighbours layers is almost the same and/or are similarly sensitive to additional carriers. Such a situation often takes place for GaAs-based structures grown on SI-type GaAs substrate. In this case possible OFs are very weak or are not observed in PR spectra. According to our experience, the OFs are very rarely observed for semiconductor structures grown on SI-type GaAs substrate. In most samples, which we have measured, the intensity of OFs was below the detection limit of our PR setup ($\Delta R/R < 10^{-6}$). However, for some samples the OF signal can be quite strong. An example of such a situation is shown in Fig. 22. In this case, optical transitions in GaAsSb-GaInAs/GaAs QW can be also resolved in PR

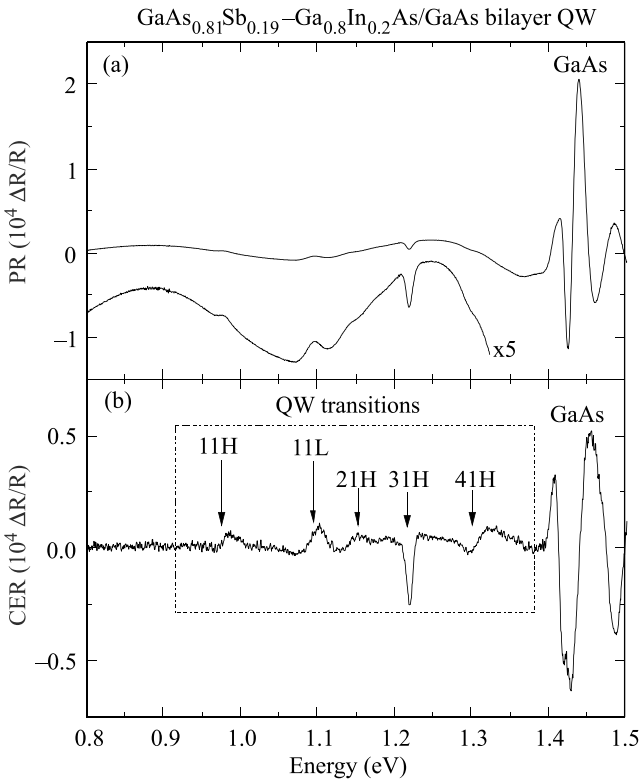

Fig. 22. Room temperature photoreflectance (a) and contactless electroreflectance (b) spectra of $GaAs_{0.81}Sb_{0.19}$-$Ga_{0.8}In_{0.2}As$/GaAs bilayer QW structure.

spectra and their energies can be extracted from these spectra as well, see details in Ref. 70. However, these transitions are much better visible in CER spectra, see Fig. 22(b).

According to our experience and the study of other authors [71,72] the ratio of OFs and a PR signal related to optical transitions (e.g., QW transitions) depends on many factors: temperature, wavelength and frequency of a modulated beam, phase of the lock-in detection and an additional illumination of the sample. In general, our investigations confirm that the ratio varies with mentioned parameters. However, we have found a lot of samples for which we are not able to obtain such an optimal ratio for these two signals. For these samples an analysis of PR features related to QW transitions is difficult. CER spectroscopy has this advantage that it gives a possibility to investigate weak optical transitions (QD and/or QW transitions) in such samples.

5. Conclusions

Experimental set-up for measurements of CER spectra in low dimensional semiconductor heterostructures and theoretical approaches to analyse experimental data have been described in this review paper. In addition, examples of application of CER spectroscopy to study various issues in low dimensional semiconductor structures have been presented and discussed. For QW structures it has been shown that CER spectroscopy supported by theoretical calculations can be used to determine the band structure of the investigated QW including the number of confined states and the band offset at QW interfaces. For QD and QDash structures it has been shown that CER spectroscopy is able to probe optical transitions in QDs (QDashes) as well as optical transitions in the wetting layer. The application of CER spectroscopy is also very fruitful in QDs (QDashes) embedded in a QW since the band structure of the surrounded QW can be determined experimentally. For QDs/QDashes coupled with a QW it is possible to investigate the coupling between the QD/QDash layer and the QW. Moreover for all low dimensional structures it is possible to probe by CER spectroscopy the energy gap of quantum barrier that is impossible in emission experiments like PL. Finally, it has been also clearly shown that CER spectroscopy is OF free which is usually observed in PR spectra measured for QD and QW structures grown on n-type GaAs substrates.

Acknowledgements

The authors acknowledge Alfred Forchel from Wurzburg University, Jean-Christophe Harmand from Laboratory for Photonics and Nanostructures at CNRS, Klaus Ploog from Paul-Drude-Institute, Mariusz Rudzinski from the Institute for Technology of Electronic Materials, their coworkers, and other our colleagues for delivering samples for CER studies as well as the COST Action MP0805 and the Ministry of Science and Higher Education (MNiSzW) grant related to this action (No. DPN/N125/ COST/2009) for their financial support.

References

1. O.J. Glembocki and B.V. Shanabrook, "Photoreflectance spectroscopy of microstructures", *Semiconductors and Semimetals* Vol. **36**, p. 221, edited by D.G. Seiler and C.L. Littler, Academic Press, New York, 1992.
2. F.H. Pollak, "Modulation spectroscopy of semiconductors and semiconductor microstructures" in M. Balkanski, *Handbook on Semiconductors*, Vol. **2**, p. 527, edited by Elsevier Science B.V., Amsterdam, 1994.
3. J. Misiewicz, P. Sitarek, and G. Sek, "Photoreflectance spectroscopy of low-dimensional semiconductor structures", *Opto-Electron. Rev.* **8**, 1 (2000).
4. J. Misiewicz, P. Sitarek, G. Sek, and R. Kudrawiec, "Semiconductor heterostructures and device structures investigated by photo-reflectance spectroscopy", *Mater. Sci.* **21**, 263 (2003).
5. R. Kudrawiec, "Application of contactless electroreflectance to III-nitrides", *Phys. Stat. Sol. (b)* **247**, 1616 (2010).
6. X. Yin and F.H. Pollak, "Novel contactless mode of electroreflectance", *Appl. Phys. Lett.* **59**, 2305 (1991).
7. R. Kudrawiec, H.B. Yuen, S.R. Bank, H.P. Bae, M.A. Wistey, J.S. Harris, M. Motyka, and J. Misiewicz, "Contactless electroreflectance approach to study the Fermi level position in GaInNAs/GaAs quantum wells", *J. Appl. Phys.* **102**, 113501 (2007).
8. R. Kudrawiec, E. Tschumak, J. Misiewicz, and D.J. As, "Contactless electroreflectance study of Fermi-level pinning

at the surface of cubic GaN", *Appl. Phys. Lett.* **96**, 241904 (2010).
9. R. Kudrawiec, M. Gladysiewicz, J. Misiewicz, V.M. Korpijarvi, J. Pakarinen, P. Laujjanen, A. Laakso, M. Guina, M. Dumitrescu, and M. Pessa, "Contactless electroreflectance study of band bending in Be-doped GaInNAs/GaAs quantum wells: The origin of photoluminescence enhancement", *Appl. Phys. Lett.* **97**, 021902 (2010).
10. M. Gladysiewicz, R. Kudrawiec, J. Misiewicz, G. Cywinski, M. Siekacz, P. Wolny, and C. Skierbiszewski, "The surface boundary conditions in GaN/AlGaN/GaN transistor heterostructures", *Appl. Phys. Lett.* **98**, 231902 (2011).
11. R. Kudrawiec, M. Motyka, M. Gladysiewicz, J. Misiewicz, J.A. Gupta, and G.C. Aers, "Contactless electroreflectance of GaN_yAs_{1-y}/GaAs multi quantum wells: The conduction band offset and electron effective mass issues", *Solid State Commun.* **138**, 365 (2006).
12. R. Kudrawiec, H.B. Yuen, S.R. Bank, H.P. Bae, M.A. Wistey, J.S. Harris, M. Motyka, and J. Misiewicz, "Fermi level shift in GaInNAsSb/GaAs quantum wells upon annealing studied by contactless electroreflectance", *Appl. Phys. Lett.* **90**, 061902 (2007).
13. R. Kudrawiec, M. Gladysiewicz, J. Misiewicz, F. Ishikawa, and K.H. Ploog, "Ground and excited state transitions in as-grown $Ga_{0.64}In_{0.36}N_{0.046}As_{0.954}$ quantum wells studied by contactless electroreflectance", *Appl. Phys. Lett.* **90**, 041916 (2007).
14. R. Kudrawiec, H.B. Yuen, M. Motyka, M. Gladysiewicz, J. Misiewicz, S.R. Bank, H.P. Bae, M.A. Wistey, and J.S. Harris, "Contactless electroreflectance of GaInNAsSb/GaAs single quantum wells with indium content of 8%–32%", *J. Appl. Phys.* **101**, 013504 (2007).
15. R. Kudrawiec, H.B. Yuen, S.R. Bank, H.P. Bae, M.A. Wistey, J.S. Harris, M. Motyka, and J. Misiewicz, "On the Fermi level pinning in as-grown GaInNAs(Sb)/GaAs quantum wells with indium content of 8%–32%", *J. Appl. Phys.* **104**, 033526 (2008).
16. R. Kudrawiec, P. Poloczek, J. Misiewicz, H.P. Bae, T. Sarmiento, S.R. Bank, H.B. Yuen, M.A. Wistey, and J.S. Harris Jr, "Contactless electroreflectance of GaInNAsSb/GaNAs/GaAs quantum wells emitting at 1.5–1.65 μm: Broadening of the fundamental transition", *Appl. Phys. Lett.* **94**, 031903 (2009).
17. R. Kudrawiec, M. Siekacz, M. Krysko, G. Cywinski, J. Misiewicz, and C. Skierbiszewski, "Contactless electroreflectance of InGaN layers with indium content ≤ 36%: The surface band bending, band gap bowing, and Stokes shift issues", *J. Appl. Phys.* **106**, 113517 (2009).
18. R. Kudrawiec, R. Kucharski, M. Rudziński, M. Zając, J. Misiewicz, W. Strupiński, R. Doradziński, and R. Dwiliński, "Application of contactless electroreflectance to study the epi readiness of m-plane GaN substrates obtained by ammonothermal method", *J. Vac. Sci. Technol. A* **28**, L18 (2010).
19. S. Moneger, H. Qiang, F.H. Pollak, D.L. Mathine, R. Droopad, and G.N. Maracas, "Contactless electroreflectance characterization of three InGaAs quantum wells placed in a GaAs/AlGaAs resonant cavity", *Solid State Electron.* **39**, 871 (1996).
20. L. Aigouy, T. Holden, F.H. Pollak, N.N. Ledentsov, W.M. Ustinov, P.S. Kopev, and D. Bimberg, "Contactless electroreflectance of a vertically coupled quantum dot-based InAs/GaAs laser", *Appl. Phys. Lett.* **70**, 3329 (1997).
21. Y.S. Huang, W.D. Sun, F.H. Pollak, J.L. Freeouf, I.D. Calder, and R.E. Mallard, "Contactless electroreflectance characterization of GaInP/GaAs heterojunction bipolar transistor structures", *Appl. Phys. Lett.* **73**, 214 (1998).
22. W. Krystek, M. Leibovitch, W.D. Sun, F.H. Pollak, G. Gumbs, G.T. Burnham, and X. Wang, "Characterization of a graded index of refraction separate confinement heterostructure (GRINSCH) laser structure using contactless electroreflectance", *J. Appl. Phys.* **84**, 2229 (1998).
23. M. Munoz, S.P. Guo, X.C. Zhou, M.C. Tamargo, Y.S. Huang, C. Trallero-Giner, and A.H. Rodriguez, "Contactless electroreflectance of CdSe/ZnSe quantum dots grown by molecular beam epitaxy", *Appl. Phys. Lett.* **83**, 4399 (2003).
24. L. Malikova, F.H. Pollak, R.A. Masut, P. Desjardins, and Lev G. Mourokh, "Temperature dependent contactless electroreflectance study of intersubband transitions in a self-assembled InAs/InP (001) quantum dot structure", *J. Appl. Phys.* **94**, 4995 (2003).
25. P. Jin, X.Q. Meng, Z.Y. Zhang, C.M. Li, B. Xu, F.Q. Liu, Z.G. Wang, Y.G. Li, C.Z. Zhang, and S.H. Pan, "Effect of InAs quantum dots on the Fermi level pinning of undoped-n^+ type GaAs surface studied by contactless electroreflectance", *J. Appl. Phys.* **93**, 4169 (2003).
26. M. Munoz, H. Lu, S. Gua, X. Zhou, M.C. Tamargo, F.H. Pollak, Y.S. Huang, C. Trallero-Giner, and A.H. Rodriguez, "Contactless electroreflectance studies of II-VI nanostructures grown by molecular beam epitaxy", *Phys. Stat. Sol.* **241**, 546 (2004).
27. V.V. Chaldyshev, A.S. Shkolnik, V.P. Evtikhiev, and T. Holden, "Optical reflection and contactless electroreflection from GaAlAs layers with periodically arranged GaAs quantum wells", *Semiconductors* **40**, 1432 (2006).
28. H.P. Hsu, A. Korotcov, Y.S. Huang, W.C. Chen, Y.K. Su, and K.K. Tiong, "Contactless electroreflectance and photoluminescence study of highly strained InGaAs(Sb) double quantum wells", *Phys. Stat. Sol.* (a) **204**, 373 (2007).
29. R. Kudrawiec and J. Misiewicz, "Photoreflectance and contactless electroreflectance measurements of semiconductor structures by using bright and dark configurations", *Rev. Sci. Instr.* **80**, 096103 (2009).
30. R. Kudrawiec and J. Misiewicz, "Photoreflectance spectroscopy of semiconductor structures at hydrostatic pressure: a comparison of GaInAs/GaAs and GaInNAs/GaAs single quantum wells", *Appl. Surf. Sci.* **253**, 80 (2006).
31. D.E. Aspnes, "Third-derivative modulation spectroscopy with low-field electroreflectance", *Surf. Sci.* **37**, 418 (1973).
32. D.E. Aspnes and A.A. Studna, "Schottky-Barrier Electroreflectance: Application to GaAs", *Phys. Rev.* ***B*****7**, 4605 (1973).
33. D.E. Aspnes, "Band nonparabolicities, broadening, and internal field distributions: The spectroscopy of Franz-Keldysh oscillations", *Phys. Rev.* ***B*****10**, 4228 (1974).
34. D.E. Aspnes, *Handbook on Semiconductors* Vol. 2, p 109, edited M. Balkanski, North Holland, Amsterdam, 1980.
35. B.V. Shanabrook, O.J. Glembocki, and W.T. Beard, "Photoreflectance modulation mechanisms in GaAs-$Al_xGa_{1-x}As$ multiple quantum wells", *Phys. Rev. B* **35**, 2540 (1987).
36. O.J. Glembocki, "Modulation spectroscopy of semiconductor materials, interfaces, and microstructures: an overview", *Proc. SPIE* **1286**, 2, San Diego (1990).
37. H. Shen and F.H. Pollak, "Generalized Franz-Keldysh theory of electromodulation", *Phys. Rev.* ***B*****42**, 7097 (1990).

38. R. Kudrawiec, P. Podemski, M. Motyka, J. Misiewicz, J. Serafińczuk, A. Somers, J.P. Reithmaier, and A. Forchel, "Electromodulation spectroscopy of $In_{0.53}Ga_{0.47}As/In_{0.53}Ga_{0.23}Al_{0.24}As$ quantum wells", *Superlattice. Microst.* **46**, 425 (2009).
39. I. Vurgaftman, J.R. Meyer, and L.R. Ram-Mohan, "Band parameters for III–V compound semiconductors and their alloys", *J. Appl. Phys.* **89**, 5815 (2001) and references therein.
40. R.F. Kopf, H.P. Wei, A.P. Perley, and G. Livescu, "Electron effective mass and band-gap dependence on alloy composition of $Al_yGa_xIn_{1-y-x}As$, lattice matched to InP", *Appl. Phys. Lett.* **60**, 2386 (1992).
41. A. Ramam and S.J. Chua, "Features of InGaAlAs/InP heterostructures", *J. Vac. Sci. Technol.* ***B*16**, 565 (1998).
42. R. Kudrawiec and J. Misiewicz, "Evidence for Fermi level shift in GaInAs/GaAs quantum well upon nitrogen incorporation", *Solid State Commun.* **150**, 227 (2010).
43. W. Shan, W. Walukiewicz, J.W. Ager III, E.E. Haller, J.F. Geisz, D.J. Friedman, J.M. Olson, and S.R. Kurtz, "Band Anticrossing in GaInNAs Alloys", *Phys. Rev. Lett.* **82**, 1221 (1999).
44. J. Misiewicz, R. Kudrawiec, K. Ryczko, G. Sęk, A. Forchel, J.C. Harmand, and M. Hammar, "Photoreflectance investigations of the energy level structure in GaInNAs-based quantum wells", *J. Phys.: Condens. Mat.* **16**, 3071 (2004).
45. W. Walukiewicz, "Intrinsic limitations to the doping of wide-gap semiconductors", *Physica* ***B*302**, 12 (2001).
46. R. Kudrawiec, S.R. Bank, H.B. Yuen, M.A. Wistey, L.L. Goddard, J.S. Harris, M. Gladysiewicz, M. Motyka, and J. Misiewicz, "Conduction band offset for $Ga_{0.62}In_{0.38}N_xAs_{0.991-x}Sb_{0.009}/GaN_xAs_{1-x}$/GaAs system with the ground state transition at 1.5-1.65 μm", *Appl. Phys. Lett.* **90**, 131905 (2007).
47. R. Kudrawiec, J. Andrzejewski, J. Misiewicz, D. Gollub, and A. Forchel, "Photoreflectance spectroscopy of step-like GaInNAs/GaInNAs/GaAs quantum wells", *Phys. Stat. Sol. (a)* **202**, 1255 (2005).
48. M. Motyka, G. Sek, R. Kudrawiec, J. Misiewicz, L.H. Li, and A. Fiore, "On the modulation mechanism in photoreflectance of an ensemble of self assembled InAs/GaAs quantum dots", *J. Appl. Phys.* **100**, 073502 (2006).
49. G. Sek, M. Motyka, R. Kudrawiec, J. Misiewicz, F. Lelarge, B. Rousseau, and G. Patriarche, "Modulated reflectivity probing of quantum dot and wetting layer states in InAs/GaInAsP/InP quantum dot laser structures", *Phys. Stat. Sol. (a)* **204**, 496 (2007).
50. R. Kudrawiec, M. Motyka, J. Misiewicz, A. Somers, R. Schwertberger, J.P. Reithmaier, A. Forchel, A. Sauerwald, T. Kümmell, and G. Bacher, "Contactless electroreflectance of $InAs/In_{0.53}Ga_{0.23}Al_{0.24}As$ quantum dashes grown on InP substrate: Analysis of the wetting layer transition", *J. Appl. Phys.* **101**, 013507 (2007).
51. W. Rudno-Rudzinski, G. Sęk, J. Misiewicz, T.E. Lamas, and A.A. Quivy, "The formation of self-assembled InAs/GaAs quantum dots emitting at 1.3 μm followed by photoreflectance spectroscopy", *J. Appl. Phys.* **101**, 073518 (2007).
52. C. Gilfert, E.-M. Pavelescu, and J.P. Reithmaier, "Influence of the As_2/As_4 growth modes on the formation of quantum dot-like InAs islands grown on InAlGaAs/InP (100)", *Appl. Phys. Lett.* **96**, 191903 (2010).
53. M. Motyka, R. Kudrawiec, G. Sęk, J. Misiewicz, I.L. Krestnikov, S. Mikhrin, and A. Kovsh, "Room temperature contactless electroreflectance characterization of InGaAs/InAs/GaAs quantum dot wafers", *Semicond. Sci. Technol.* **21**, 1402 (2006).
54. M. Motyka, R. Kudrawiec, G. Sek, J. Misiewicz, D. Bisping, B. Marquardt, A. Forchel, and M. Fischer, "Contactless electroreflectance investigation of energy levels in a 1.3 μm emitting laser structure with the gain medium composed of InAsN quantum dots embedded in GaInNAs/GaAs quantum wells", *Appl. Phys. Lett.* **90**, 221112 (2007).
55. W. Rudno-Rudziński, R. Kudrawiec, G. Sęk, J. Misiewicz, A. Somers, R. Schwertberger, J. P. Reithmaier, and A. Forchel, "Photoreflectance investigation of InAs quantum dashes embedded in $In_{0.53}Ga_{0.47}As/In_{0.53}Ga_{0.23}Al_{0.24}As$ quantum well grown on InP substrate", *Appl. Phys. Lett.* **88**, 141915 (2006).
56. S. Hein, S. Hofling, and A. Forchel, "Modulation Bandwidth and Linewidth Enhancement Factor of High-Speed 1.55-μm Quantum-Dash Lasers", *IEEE Photon. Technol. Lett.* **21**, 528 (2009) and references therein.
57. Kudrawiec, G. Sęk, M. Motyka, J. Misiewicz, A. Somers, S. Höfling, L. Worschech, and A. Forchel, "Contactless electroreflectance of optical transitions in tunnel-injection structures composed of an $In_{0.53}Ga_{0.47}As/In_{0.53}Ga_{0.23}Al_{0.24}As$ quantum well and InAs quantum dashes", *J. Appl. Phys.* **108**, 086106 (2011).
58. G. Sek, P. Poloczek, P. Podemski, R. Kudrawiec, J. Misiewicz, A. Somers, S. Hein, S Hofling, and A. Forchel, "Experimental evidence on quantum well-quantum dash energy transfer in tunnel injection structures for 1.55 μm emission", *Appl. Phys. Lett.* **90**, 081915 (2007).
59. W. Rudno-Rudziński, K. Ryczko, G. Sęk, R. Kudrawiec, J. Misiewicz, A. Somers, R. Schwertberger, J.P. Reithmaier, and A. Forchel, "Optically probed wetting layer in InAs/InGaAlAs/InP quantum dash structures", *Appl. Phys. Lett.* **86**, 101904 (2005).
60. R. Kudrawiec, P. Sitarek, J. Misiewicz, S.R. Bank, H.B. Yuen, M.A. Wistey, and J.S. Harris Jr, "Interference effects in electromodulation spectroscopy applied to GaAs-based structures: A comparison of photoreflectance and contactless electroreflectance", *Appl. Phys. Lett.* **86**, 091115 (2005).
61. R. Kudrawiec, M. Motyka, M. Gladysiewicz, P. Sitarek, and J. Misiewicz, "Photoreflectance and contactless electroreflectance spectroscopy of GaAs-based structures: The below band gap oscillation features", *Appl. Surf. Sci.* **253**, 266 (2006).
62. M. Motyka, R. Kudrawiec, and J. Misiewicz, "On the deepness of contactless electroreflectance probing in semiconductor structures", *Phys. Stat. Sol. (a)* **204**, 354 (2007).
63. P.J. Klar, C.M. Townsley, D. Wolverson, J.J. Davies, D.E. Ashenford, and B. Lunn, "Photomodulated reflectivity of $ZnTe/Zn_{1-x}Mn_xTe$ multiple quantum wells with below--bandgap excitation", *Semicond. Sci. Technol.* **10**, 1568 (1995).
64. R. Kudrawiec, M. Rudziński, J. Serafinczuk, M. Zając, and J. Misiewicz, "Photoreflectance study of exciton energies and linewidths for homoepitaxial and heteroepitaxial GaN layers", *J. Appl. Phys.* **105**, 093541 (2009).
65. J. Misiewicz, G. Sęk, R. Kudrawiec, and P. Sitarek, "Photomodulated reflectance and transmittance: optical characterization of novel semiconductor materials and device structures", *Thin Solid Films* **450**, 14 (2004).
66. R. Kudrawiec, M. Syperek, M. Motyka, J. Misiewicz, R. Paszkiewicz, B. Paszkiewicz, and M. Tłaczała, "Contactless electromodulation spectroscopy of AlGaN/GaN heterostruc-

tures with a two-dimensional electron gas: A comparison of photoreflectance and contactless electroreflectance", *J. Appl. Phys.* **100**, 013501 (2006).
67. M. Motyka, R. Kudrawiec, M. Syperek, J. Misiewicz, M. Rudziński, P. Hageman, and P.K. Larsen, "Screening effect in contactless electroreflectance spectroscopy observed for AlGaN/GaN heterostructures with 2DEG", *Thin Solid Films* **515**, 4662 (2007).
68. R. Kudrawiec, E.-M. Pavelescu, J. Andrzejewski, J. Misiewicz, A. Gheorghiu, T. Jouhti, and M. Pessa, "The energy--fine structure of GaInNAs/GaAs multiple quantum wells grown at different temperatures and post-grown annealed", *J. Appl. Phys.* **96**, 2909 (2004).
69. R. Kudrawiec, E.-M. Pavelescu, J. Wagner, G. Sęk, J. Misiewicz, M. Dumitrescu, J. Konttinen, A. Gheorghiu, and M. Pessa, "The photoreflectance evidence of multiple band gaps in dilute GaInNAs layers lattice–matched to GaAs", *J. Appl. Phys.* **96**, 2576 (2004).
70. R. Kudrawiec, G. Sęk, K. Ryczko, and J.C. Harmand, "Photoreflectance investigations of oscillator strength and broadening of optical transitions for GaAsSb–GaInAs/GaAs bilayer quantum wells", *Appl. Phys. Lett.* **84**, 3453 (2004).
71. N. Kallergi, B. Roughani, J. Aubel, and S. Sundaram, "Correlation of interference effects in photoreflectance spectra with GaAs homolayer thickness", *J. Appl. Phys.* **68**, 4656 (1990).
72. H.K. Lipsanen and V.M. Airaksinen, "Interference effects in photoreflectance of epitaxial layers grown on semi-insulating substrates", *Appl. Phys. Lett.* **63**, 2863 (1993).